

Exactly solvable models of growing interfaces and lattice gases: the Arcetri models, ageing and logarithmic sub-ageing

Xavier Durang^{a,b1} and Malte Henkel^{c,d,e2}

^aSchool of Physics, Korea Institute for Advanced Study, Seoul 130-722, Korea

^bDepartment of Physics, University of Seoul, Seoul 02504, Korea

^cRechnergestützte Physik der Werkstoffe, Institut für Baustoffe (IfB),
ETH Zürich, Stefano-Franscini-Platz 3, CH – 8093 Zürich, Switzerland

^dGroupe de Physique Statistique, Département de Physique de la Matière et des Matériaux,
Institut Jean Lamour (CNRS UMR 7198), Université de Lorraine Nancy, B.P. 70239,
F – 54506 Vandœuvre lès Nancy Cedex, France³

^eCentro de Física Teórica e Computacional, Universidade de Lisboa,
P–1749-016 Lisboa, Portugal

Abstract

Motivated by an analogy with the spherical model of a ferromagnet, the three Arcetri models are defined. They present new universality classes, either for the growth of interfaces, or else for lattice gases. They are distinct from the common Edwards-Wilkinson and Kardar-Parisi-Zhang universality classes. Their non-equilibrium evolution can be studied from the exact computation of their two-time correlators and responses. The first model, in both interpretations, has a critical point in any dimension and shows simple ageing at and below criticality. The exact universal exponents are found. The second and third model are solved at zero temperature, in one dimension, where both show logarithmic sub-ageing, of which several distinct types are identified. Physically, the second model describes a lattice gas and the third model interface growth. A clear physical picture on the subsequent time- and length-scales of the sub-ageing process emerges.

PACS numbers: 05.40.-a, 05.70.Ln, 81.10.Aj, 02.50.-r, 68.43.De

¹e-mail: xdurang1@uos.ac.kr

²e-mail: malte.henkel@univ-lorraine.fr

³permanent address;

after 1st of Januar 2018: Laboratoire de Physique et Chimie Théoriques (CNRS UMR), Université de Lorraine Nancy, B.P. 70239, F – 54506 Vandœuvre-lès Nancy Cedex, France

1 Introduction

The physics of the growth of interfaces is a paradigmatic example of the emergence of non-equilibrium cooperative phenomena, with widespread applications in domains as different as deposition of atoms on a surface, solidification, flame propagation, population dynamics, crack propagation, chemical reaction fronts or the growth of cell colonies [3, 32, 53, 52, 17, 81, 77, 82]. Several universal growth and roughness exponents characterise the morphology of the growing interface and the time-dependent properties are quite analogous to phenomena encountered in the physical ageing in glassy and non-glassy systems [20, 37, 78]. Several universality classes of interface growth have been identified, the best-known of these are characterised in terms of stochastic equations for the height profile $h = h(t, \mathbf{r})$

$$\begin{cases} \partial_t h = \nu \nabla^2 h + \eta & ; \text{Edwards-Wilkinson EW [23]} \\ \partial_t h = \nu \nabla^2 h + \frac{\mu}{2} (\nabla h)^2 + \eta & ; \text{Kardar-Parisi-Zhang KPZ [46]} \end{cases} \quad (1.1)$$

where ∇ is the spatial gradient, η is a centred gaussian white noise, with covariance

$$\langle \eta(t, \mathbf{r}) \eta(t', \mathbf{r}') \rangle = 2\nu T \delta(t - t') \delta(\mathbf{r} - \mathbf{r}') \quad (1.2)$$

and ν, μ, T are material-dependent constants.

While the exact solution of the EW-equation is straightforward, extracting the long-distance and/or long-time properties of interfaces in the KPZ-class is considerably more difficult and several aspects of the problem still remain unresolved. Remarkable progress has been achieved in recent years on the exact solution of the KPZ-equation in $d = 1$ dimension. In particular, several spatial correlators have been found exactly and a deep relationship of the probability distribution $\mathcal{P}(h)$ of the fluctuation $h - \bar{h}$ with the extremal value statistics of the largest eigenvalue of random matrices has been derived, see [69, 12, 13, 43, 33, 34, 48]. Very remarkably, these mathematical results could be confirmed experimentally, in several physically distinct systems [73, 40, 74, 75, 83, 36, 35, 41, 2, 76]. Still, this impressive progress seems to rely on specific properties of the one-dimensional case. Therefore, one might wonder if further classes of exactly solvable models of interface growth could be defined, distinct from both the EW- as well as the KPZ-universality class, and what physical insight the study of such models might provide.

Indeed, a new class of models can be defined, with the help of some inspiration from the definition of the well-studied *spherical model* of a ferromagnet [7, 57]. Therein, the traditional Ising spins $\sigma_i = \pm 1$, attached to the sites i of a lattice with \mathcal{N} sites, are replaced by continuous spins $S_i \in \mathbb{R}$ and subject to the ‘*spherical constraint*’ $\sum_i S_i^2 = \mathcal{N}$. A conventional nearest-neighbour interaction leads to an exactly solvable model, which undergoes a non-trivial phase transition in $2 < d < 4$ dimensions [7, 44]. The relaxational properties can be likewise analysed exactly, see e.g. [67, 14, 18, 19, 29, 27, 65, 22, 26, 30]. In order to identify an analogy with growing interfaces, we restrict here to $d = 1$ dimensions for simplicity. Consider a lattice representation of the KPZ-class where the height differences between two nearest neighbours obey the so-called RSOS constraint $h_{i+1}(t) - h_i(t) = \pm 1$. It is well-established that in the continuum limit this model is described by the KPZ-equation [3, 32, 77], see [8] for a rigorous derivation. The dynamic deposition rule is sketched in figure 1, which makes it clear that in this kind of lattice model, the slopes $u_{i+1/2}(t) := h_{i+1}(t) - h_i(t)$ should be considered as the analogues of the Ising spins $\sigma_i = \pm 1$ in ferromagnets. For the slopes, in the continuum limit,

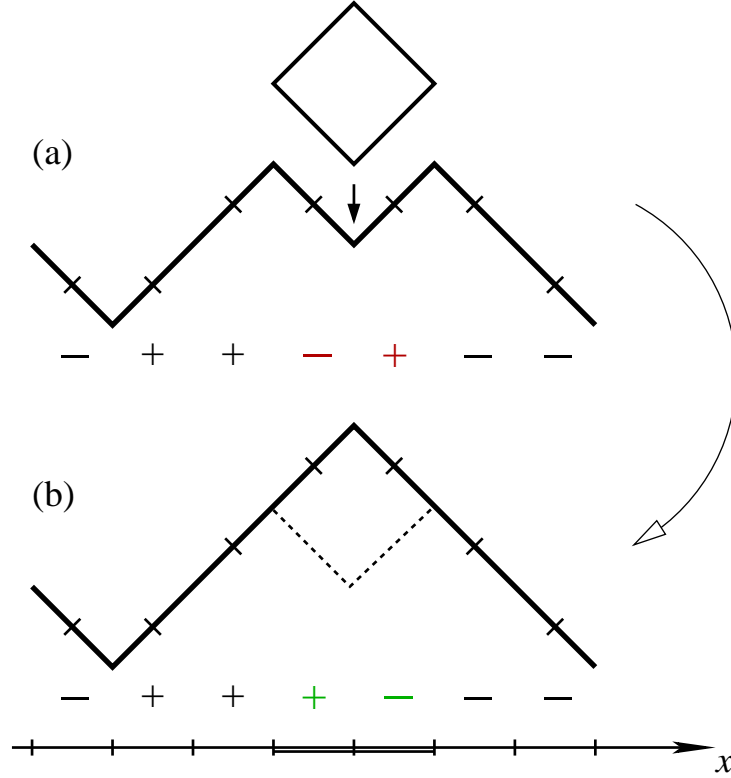


Figure 1: Illustration of the growth of an interface obeying the RSOS condition. In (a), the interface is shown before the adsorption of a particle and in (b), the same interface is shown after the adsorption process. Below the interfaces (a) and (b), the slopes $u_j = h_{j+\frac{1}{2}} - h_{j-\frac{1}{2}}$, defined on the dual lattice $j \in \mathbb{Z} + \frac{1}{2}$ are indicated. The adsorption process is described by a move $(-+) \rightarrow (+-)$ in terms of the slopes, where the participating slopes are indicated in red before the adsorption (a) and in green afterwards (b).

from the KPZ-equation follows the (noisy) Burgers equation [10] (for a discrete analogue, see [4])

$$\partial_t u = \nu \nabla^2 u + \mu u \nabla u + \nabla \eta \quad (1.3)$$

A ‘spherical model variant’ of the KPZ-universality class now stipulates to relax the RSOS-constraints $u_i = \pm 1$ to a ‘spherical constraint’ $\sum_i \langle u_i^2 \rangle = \mathcal{N}$ [39].¹ However, for growing interfaces several equivalent descriptions can give rise to several new models, which may or may not be in the same universality class. Heuristically, the following possibilities may occur:

1. One may start from the Burgers equation and replace its non-linearity as follows

$$\partial_t u = \nu \nabla^2 u + \mu u \nabla u + \nabla \eta \quad \mapsto \quad \partial_t u = \nu \nabla^2 u + \mathfrak{z}(t) u + \nabla \eta \quad (1.4)$$

with a Lagrange multiplier $\mathfrak{z}(t) \sim \langle \nabla u \rangle$ which might be seen as some kind of ‘averaged curvature’ of the interface. Its value is determined by the mean spherical constraint² $\sum \langle u^2 \rangle = \mathcal{N}$. This

¹An old observation by Oono and Puri [63] gives additional motivation: treating the Allen-Cahn equation of phase-ordering, after a quench to $T < T_c$, along the lines of the celebrated Ohta-Jasnow-Kawasaki approximation, but for a *finite* thickness of the domain boundaries, leads to a kinetic equation in the universality class of the spherical model.

²In this section, the average $\langle \cdot \rangle$ is understood to be taken over both the ‘thermal’ as well as the ‘initial’ noise.

is the ‘*first Arcetri model*’, defined³ and analysed in [39].⁴ In any dimension $d > 0$, there is a ‘critical temperature’ $T_c(d) > 0$ such that long-range correlations build up for $T \leq T_c(d)$. At the critical point $T = T_c(d)$, the interface is rough for $d < 2$ and is smooth for $d > 2$. For $T < T_c(d)$, the interface is always rough. The model is also related to the gaps in the spectra of random matrices [28] and to the spherical spin glass [19].

2. An alternative way to treat the Burgers equations might proceed as follows

$$\partial_t u = \nu \nabla^2 u + \mu u \nabla u + \nabla \eta \quad \mapsto \quad \partial_t u = \nu \nabla^2 u + \mathfrak{z}(t) \nabla u + \nabla \eta \quad (1.5)$$

where the Lagrange multiplier $\mathfrak{z}(t) \sim \langle u \rangle$ might now be viewed as some kind of ‘averaged slope’. Its value is again determined by the constraint $\sum \langle u^2 \rangle = \mathcal{N}$. This would define a ‘*second Arcetri model*’.

3. Finally, we might have started directly from the KPZ equation

$$\partial_t h = \nu \nabla^2 h + \frac{1}{2} \mu (\nabla h)^2 + \eta \quad \mapsto \quad \partial_t h = \nu \nabla^2 h + \mathfrak{z}(t) \nabla h + \eta \quad (1.6)$$

where $\mathfrak{z}(t) \sim \langle \nabla h \rangle$ might again be interpreted as an ‘averaged slope’ and will be found from a constraint $\sum \langle (\nabla h)^2 \rangle = \mathcal{N}$. This would be a ‘*third Arcetri model*’.

However, such a simplistic procedure would lead to undesirable properties of the height and slope profiles in the stationary state, as well as to internal inconsistencies. We shall therefore reconsider this correspondence carefully in section 2, where the precise definitions of the second and third Arcetri model will be given.

In one spatial dimension, the slope profile has an interesting relationship with the dynamics of interacting particles. To see this, write the slope as $u(t, r) = 1 - 2\varrho(t, r)$, where $\varrho(t, r)$ denotes the particle-density at time $t \in \mathbb{R}_+$ and position $r \in \mathbb{R}$. In the KPZ universality class, when on the lattice the RSOS-constraint $u(t, r) = \pm 1$ holds, denote by \bullet an occupied site with $\varrho = 1$ and by \circ an empty site with $\varrho = 0$. Then the only admissible reaction between neighbouring sites is the directed jump $\bullet\circ \longrightarrow \circ\bullet$. The stochastic process described by these interacting particles is a *totally asymmetric exclusion process* (TASEP), see e.g. [56, 31, 21, 58], which is integrable via the Bethe ansatz. Here, we are interested in the situation when the exact RSOS-constraint is relaxed to the mean ‘spherical constraint’ $\langle \sum_r u(t, r)^2 \rangle = \mathcal{N}$. In terms of the noise-averaged particle-density, this becomes

$$\sum_r \langle \varrho(t, r) \rangle = \sum_r \langle \varrho(t, r)^2 \rangle \quad (1.7)$$

where the sums run over all sites of the lattice. Hence, on any site, neither $\langle \varrho(t, r) \rangle$ nor the difference $\langle \varrho(t, r) \rangle - 1$ can become very large, since the spherical constraint prohibits the condensation of almost all particles onto a very small number of sites. In particular, if one takes a spatially translation-invariant initial condition, then spatial translation-invariance is kept for all times. Because of the constraint (1.7), the average (position-independent) particle-density

$$\rho(t) := \frac{1}{\mathcal{N}} \sum_r \langle \varrho(t, r) \rangle \geq 0 \quad (1.8)$$

is always non-negative. We point out that while the non-averaged density variable $\varrho(t, r) \in \mathbb{R}$ has no immediate physical interpretation, the constraint (1.7) guarantees that the measurable *disorder-averaged observables* takes physically reasonable values.

³The name comes from the location of the Galileo Galilei Institute of Physics, where this model was conceived.

⁴It can be shown that $\mathfrak{z}(t) \sim t^{-1}$ for sufficiently long times, whenever $T \leq T_c(d)$.

Table 1: Non-equilibrium exponents, as defined in the text, for several universality classes of growing-interface models. The ARCETRI 1H class at $T = T_c$ for $d > 2$ is identical to the EW class [23, 68, 11, 42, 48]. For the ARCETRI 3 class, there are three distinct logarithmic sub-ageing scaling regimes, which are characterised by the value of the logarithmic sub-ageing parameter ϑ as indicated. For $\vartheta < 1$, the autoresponse function does not display scaling behaviour, as indicated by DNS (**d**oes **n**ot **s**cale). For empty entries, no estimate is known. The initial state is flat on average, with uncorrelated heights.

model	d	a	b	λ_C	λ_R	z	β	Ref.
KPZ	1	$-1/3$	$-2/3$	1	1	$3/2$	$1/3$	[46, 51, 45, 38]
KPZ	2		-0.483	$1.91(6)$		$1.61(2)$	$0.241(1)$	[36]
KPZ	2	$0.30(1)$	$-0.483(3)$	$1.97(3)$	$2.04(3)$	$1.61(2)$	$0.2415(15)$	[62]
KPZ	2	$0.24(1)$	$-0.483(3)$	$1.97(3)$	$2.00(6)$	$1.61(2)$	$0.2415(15)$	[47]
KPZ	2	$0.24(1)$	$-0.4828(4)$	$1.98(5)$ $2.01(2)$	$2.00(6)$	$1.611(3)$	$0.2414(2)$	[48]
ARCETRI 1H $T = T_c$	< 2	$\frac{d}{2} - 1$	$\frac{d}{2} - 1$	$\frac{3d}{2} - 1$	$\frac{3d}{2} - 1$	2	$\frac{1}{4}(2 - d)$	[39]
ARCETRI 1H $T = T_c$	> 2	$\frac{d}{2} - 1$	$\frac{d}{2} - 1$	d	d	2	0	[39]
ARCETRI 1H $T < T_c$	d	$\frac{d}{2} - 1$	-1	$\frac{d}{2} - 1$	$\frac{d}{2} - 1$	2	$\frac{1}{2}$	[39]
ARCETRI 3 $T = 0$	1	$-\frac{1}{2}$	0	0	1	2	0	$\vartheta > 1$
ARCETRI 3 $T = 0$	1	DNS	0	0	DNS	2	0	$\frac{1}{2} < \vartheta < 1$
ARCETRI 3 $T = 0$	1	DNS	0	∞	DNS	2	0	$\vartheta = \frac{1}{2}$

The long-time non-equilibrium relaxation behaviour is analysed as follows. In models of interface growth, one usually starts from a flat, horizontal interface with uncorrelated heights [3, 32, 68, 38, 36, 62, 39, 47, 48, 49]. One then studies the average height $\langle h(t, r) \rangle \sim t^\beta$, the interface width $w^2(t) = \langle (h(t, r) - \langle h(t, r) \rangle)^2 \rangle \sim t^{2\beta}$, and the two-time height autocorrelator and auto-response of the height with respect to a change in the height

$$C(t, s) := \langle (h(t, r) - \langle h(t, r) \rangle) (h(s, r) - \langle h(s, r) \rangle) \rangle = s^{-b} f_C \left(\frac{t}{s} \right) \quad (1.9)$$

$$R(t, s) := \left. \frac{\delta \langle h(t, r) \rangle}{\delta j(s, r)} \right|_{j=0} = s^{-1-a} f_R \left(\frac{t}{s} \right) \quad (1.10)$$

The scaling forms [24] used here are those of *simple ageing* and apply in the long-time limit $t, s \rightarrow \infty$ with $y = t/s$ being kept fixed. The scaling functions are expected to have the asymptotic behaviour

$$f_C(y) \stackrel{y \gg 1}{\sim} y^{-\lambda_C/z}, \quad f_R(y) \stackrel{y \gg 1}{\sim} y^{-\lambda_R/z} \quad (1.11)$$

where z is the dynamical exponent. From these relations the exponents β and $a, b, \lambda_C, \lambda_R$ are defined. In table 1, some values of these exponents are collected.⁵ Starting from the Langevin equation (1.4) of the first Arcetri model, formulated in terms of the slopes u and using $u = \nabla h$, an analogous Langevin equation for the heights h is found, if only the spherical constraint is now written as $\sum \langle (\nabla h)^2 \rangle = \mathcal{N}$. In what follows, we shall call this the ARCETRI

⁵The 2D KPZ universality class is realised by the octahedron model [62]. For height correlators and responses, the results of the random sequential (RS) update and of the two-sublattice stochastic dynamics (SCA) update are consistent, confirming the expected universality ($\lambda_{C,RS} = 1.98(5)$, $\lambda_{C,SCA} = 2.01(2)$) [48]. Comparison with the recent result $z = 1.613(2)$ [64] gives an *a posteriori* indication of the presently achieved numerical precision.

1H *model*. Its relaxational behaviour undergoes (simple) ageing for both $T = T_c$ and for $T < T_c$, in agreement with the expected scaling forms (1.9,1.10). In appendix A, we briefly outline how to find the exponents. Logarithmic sub-scaling exponents [50] in $w(t)$ of the third Arcetri model are discussed in section 4.

The main focus of this work will be on defining (see section 2 for the precise definitions) and analysing the ‘second’ and the ‘third’ Arcetri models. At temperature $T = 0$, we shall see that the simple ageing behaviour of eqs. (1.9,1.10,1.11) does not apply. Rather, we shall find a ‘*logarithmic sub-ageing*’ behaviour,⁶ in the scaling limit where both times $t, s \rightarrow \infty$, but such that the scaling variable y of two-time scaling

$$y - 1 := \frac{t - s}{s} \ln^\vartheta \kappa_2 s \quad (1.12)$$

is being kept fixed (κ_2 is a model-dependent constant). It turns out that several types of logarithmic sub-ageing exist for the Arcetri models, which are characterised by different values of the logarithmic sub-ageing exponent $\vartheta > 0$.⁷ With the scaling variable (1.12), the asymptotic scaling forms (1.11) often remain applicable and the corresponding exponent values are quoted in tables 1 and 2. Logarithmic sub-ageing arises from the presence of several time-dependent length scales, which differ by factors logarithmic in time, a phenomenon also referred to as *multiscaling* [14]. If the autocorrelator scaling function $f_C(y)$ decays with y faster than a power-law (exponentially or stretched exponentially), the value $\lambda_C = \infty$ is quoted. See section 5 for a fuller discussion.

Analogously, if one considers a system of interacting particles, one usually assumes an initial state of uncorrelated particles (uncorrelated, flat slopes $\langle u(t, r) \rangle = 0$, in the present terminology) with an average particle density $\varrho = \langle \varrho(t, r) \rangle = \frac{1}{2}$, equivalent to a vanishing initial slope [21, 48]. One considers the two-time slope (connected) auto-correlator $C(t, s)$, which is related to the density-density autocorrelator, and the linear auto-responses $R(t, s)$, $\mathcal{R}(t, s)$ of the slope with respect to a change $k = \nabla j$ in the slope or a change j in the height, respectively

$$C(t, s) := \langle u(t, r)u(s, r) \rangle = 4 \left\langle \left(\varrho(t, r) - \frac{1}{2} \right) \left(\varrho(s, r) - \frac{1}{2} \right) \right\rangle = s^{-b} f_C \left(\frac{t}{s} \right) \quad (1.13)$$

$$R(t, s) := \left. \frac{\delta \langle u(t, r) \rangle}{\delta k(s, r)} \right|_{k=0} = s^{-1-a} f_R \left(\frac{t}{s} \right) \quad (1.14)$$

$$\mathcal{R}(t, s) := \left. \frac{\delta \langle u(t, r) \rangle}{\delta j(s, r)} \right|_{j=0} = s^{-1-a_{\mathcal{R}}} f_{\mathcal{R}} \left(\frac{t}{s} \right) \quad (1.15)$$

along with the expected behaviour of simple ageing in the scaling limit. Eq. (1.11) applies again and analogously, one anticipates $f_{\mathcal{R}}(y) \sim y^{-\lambda_{\mathcal{R}}/z}$, for $y \gg 1$. Considering numerical simulations of the 2D octahedron model, however, it appears that for the slope correlations the two update schemes RS and SCA lead to different values of the autocorrelation exponent – and this for model realisation both in the KPZ as well as in the EW universality classes [48]. The first Arcetri model with initially uncorrelated slopes will be called the *ARCETRI 1U model*. It

⁶Sub-ageing behaviour is defined by the scaling variable $y - 1 := \frac{\kappa_2(t-s)}{(\kappa_2 s)^\mu}$, where $0 < \mu < 1$ is the *sub-ageing exponent* and $\mu = 1$ gives back simple ageing [20, 79]. See [37, Tab 1.2] for a list of experimentally measured values of μ . A basic rigorous inequality excludes the case $\mu > 1$ (‘super-ageing’) [54].

⁷For $\vartheta = 0$, one is back to simple ageing

Table 2: Non-equilibrium exponents for several universality classes of lattice-gas models, where ‘octa’ stands for ‘octahedron model’, RS for random sequential update and SCA for two-sub-lattice stochastic dynamics. The model realisations in the KPZ and EW universality classes are indicated. For the ARCETRI 2 and conserved spherical classes, there are three logarithmic sub-ageing scaling regimes which are characterised by the value of the logarithmic sub-ageing parameter ϑ is indicated. For $\vartheta < 1$, the autoresponse functions do not display scaling behaviour, indicated by DNS. For empty entries, there is no estimate. The initial state has an average particle density $\varrho = \frac{1}{2}$ and uncorrelated particles.

model	d	a	$a_{\mathcal{R}}$	b	λ_C	λ_R	$\lambda_{\mathcal{R}}$	z	Ref.
TASEP	1			2/3	3			3/2	[21]
octa RS	KPZ 2			0.76(2)	3.8(2)			1.611(3)	[48]
octa SCA	KPZ 2				1.25(2)			1.611(3)	[48]
octa SCA	EW 2			1.1(2)	≈ 4			2	[48]
octa RS	EW 2			1.1(2)	1.4(4)			2	[48]
ARCETRI 1U $T = T_c$	d	$d/2$	$d/2 + 1$	$d/2$	$d + 2$	d	$d + 2$	2	
ARCETRI 1U $T < T_c$	d	$d/2 - 1$	$d/2$	0	$d/2$	$d/2$	$d/2 + 2$	2	
ARCETRI 2 $T = 0$	1	-1/2	0	0	0	1	1	2	$\vartheta > 1$
ARCETRI 2 $T = 0$	1	DNS	DNS	0	0	DNS		2	$\frac{1}{2} < \vartheta < 1$
ARCETRI 2 $T = 0$	1	DNS	DNS	0	∞	DNS		2	$\vartheta = \frac{1}{2}$
spherical $T = 0$	d	$(d - 2)/4$		0	0	$d + 2$		4	$\vartheta > 1$
spherical $T = 0$	d	DNS	DNS	0	0	DNS	DNS	4	$\frac{1}{2} < \vartheta < 1$
spherical $T = 0$	d	DNS	DNS	0	∞	DNS	DNS	4	$\vartheta = \frac{1}{2}$ [9]

is suggestive to compare the corresponding exponent values with those of the EW universality class. Some values of these exponents are listed in table 2, see appendix A for the outline of the calculations in the ARCETRI 1U model. We also include results from the spherical model with a conserved order parameter (‘model B’), at $T = 0$ [14, 9]. It also becomes apparent how much less is known about responses of the slope variables than for the height variables.

This work is organised as follows: in section 2, the second and third Arcetri model are carefully defined. Since the first Arcetri model was already studied [39], we merely outline its treatment in appendix A and quote the results in tables 1 and 2, where the two possible interpretations are taken into account. Section 3 explains the solution of the second and third models. The explicit spherical constraints and a closed form for correlators and responses are derived. In section 4, the asymptotic analysis at temperature $T = 0$ and the emergence of the different types of logarithmic sub-ageing in the second and third models is presented. We conclude in section 5 with a detailed presentation of the kinetic phase diagram and the various scales on which different aspects of logarithmic sub-ageing occur. Technical calculations are treated in several appendices. Appendix A contains a short summary of the first model, both for an interface and for a lattice gas. Appendices B and C derive the various distinct sub-ageing scaling forms of correlators and responses, respectively. Several mathematical identities are derived in appendices D and E and some basics of discrete cosine- and sine transformations are collected in appendix F.

2 The second and third Arcetri models

2.1 Preliminaries

Why are the equations (1.5,1.6) physically unsatisfactory ? In order to understand this, and in consequence the necessity for a better definition of the models, consider for a moment the behaviour of the stationary profiles, as they would follow from eqs. (1.4,1.5,1.6). Let \mathfrak{z}_∞ denote the stationary value of the Lagrange multiplier. Then the noise-averaged slope profile of the first Arcetri model (1.4) is oscillatory $u_{\text{stat}}(r) \sim \cos(r/\lambda + \varphi_0)$, with the finite wave-length $\lambda = \sqrt{\nu/\mathfrak{z}_\infty}$, as one would have expected. On the other hand, eq. (1.5) would produce a spatially strongly variable stationary slope profile $u_{\text{stat}}(r) \sim \exp(-r/r_0)$, with a finite length-scale $r_0 = \nu/\mathfrak{z}_\infty$. Finally, eq. (1.6) gives an analogous result for the stationary height profile. This is in apparent contradiction with the expectation of essentially flat profiles, both for the height as well as the slope.

2.2 Definition of the second Arcetri model

How can one formulate a physically sensible ‘spherical model variant’ of the Burgers equation ? Begin with a decomposition of the slope profile $u(t, r)$, with $r \in \mathbb{R}$, into its even and odd parts

$$u(t, r) = a(t, r) + b(t, r) \quad (2.1)$$

where

$$\begin{aligned} a(t, r) &:= \frac{1}{2} (u(t, r) + u(t, -r)) = a(t, -r) \quad \text{even} \\ b(t, r) &:= \frac{1}{2} (u(t, r) - u(t, -r)) = -b(t, -r) \quad \text{odd} \end{aligned} \quad (2.2)$$

For definiteness, we shall formulate the defining equations of motion of the *second Arcetri model* on a periodic chain of N sites. They read

$$\begin{aligned} \partial_t a_n(t) &= \nu (a_{n+1}(t) + a_{n-1}(t) - 2a_n(t)) + \frac{1}{2} \mathfrak{z}(t) (b_{n+1}(t) - b_{n-1}(t)) + \frac{1}{2} (\eta_{n+1}^-(t) - \eta_{n-1}^-(t)) \\ \partial_t b_n(t) &= \nu (b_{n+1}(t) + b_{n-1}(t) - 2b_n(t)) - \frac{1}{2} \mathfrak{z}(t) (a_{n+1}(t) - a_{n-1}(t)) - \frac{1}{2} (\eta_{n+1}^+(t) - \eta_{n-1}^+(t)) \end{aligned} \quad (2.3)$$

where $\eta_n^\pm(t) := \frac{1}{2} (\eta_n(t) \pm \eta_{N-n}(t))$ is the parity-symmetrised and -antisymmetrised white noise $\eta_n(t)$, with the moments

$$\langle \eta_n(t) \rangle = 0 \quad , \quad \langle \eta_n(t) \eta_m(t') \rangle = 2\nu T \delta_{n,m} \delta(t - t') \quad (2.4)$$

Hence one has the (anti-)symmetrised noise correlators

$$\langle \eta_n^\pm(t) \rangle = 0 \quad , \quad \langle \eta_n^\pm(t) \eta_m^\pm(t') \rangle = \nu T \delta(t - t') [\delta_{n,m} \pm \delta_{n,N-m}] \quad , \quad \langle \eta_n^\pm(t) \eta_m^\mp(t') \rangle = 0 \quad (2.5)$$

(clearly, the indices n, m are to be taken *modulo* N). The second Arcetri model will be considered as a variant of the Burgers equation and its associated TASEP. Therefore, a natural

choice of initial conditions is to admit initially uncorrelated slopes, distributed according to a gaussian, and with the moments

$$\begin{aligned}\langle\langle a_n(0) \rangle\rangle &= \langle\langle b_n(0) \rangle\rangle = 0 & , & \quad \langle\langle a_n(0)b_m(0) \rangle\rangle = 0 \\ \langle\langle a_n(0)a_m(0) \rangle\rangle &= \frac{1}{2}(\delta_{n,m} + \delta_{n,N-m}) & , & \quad \langle\langle b_n(0)b_m(0) \rangle\rangle = \frac{1}{2}(\delta_{n,m} - \delta_{n,N-m})\end{aligned}\quad (2.6)$$

The Lagrange multiplier $\mathfrak{z}(t)$ is determined from the mean spherical constraint on the slopes

$$\left\langle\left\langle\left\langle\sum_{n=1}^N (a_n(t) + b_n(t))^2\right\rangle\right\rangle\right\rangle = N \quad (2.7)$$

which is averaged over both sources of noise present in the model, as indicated by the brackets $\langle.\rangle$ for the average over η and $\langle\langle.\rangle\rangle$ for the average over the initial conditions. We stress that the even and odd parts are treated in a slightly different way. In this way, two essential properties of the Burgers equation, namely (i) the conservation law and (ii) the non-invariance under the parity transformation $x \mapsto -x$ [10, 4] are kept. The initial conditions (2.6) are natural if one wishes to interpret the slope $u(t, r) = 1 - 2\varrho(t, r)$ in terms of the density $\varrho(t, r)$ of a model of interacting particles, with the average density $\varrho = \langle\langle\langle\varrho(t, r)\rangle\rangle\rangle = \frac{1}{2}$.

Eqs. (2.3, 2.6, 2.7), together with the noise correlator (2.5), define the **second Arcetri model**.

Formally, one might also arrive at these equations by introducing a complex velocity $u = a + ib$ into the modification (1.5) of the Burgers equation, with a complex Lagrange multiplier $\mathfrak{z}(t) = \mathfrak{z}_1(t) - i\mathfrak{z}_2(t)$ and a complex noise $\eta(t, r) = i(\eta^+(t, r) - i\eta^-(t, r))$. Separating into real and imaginary parts, this would give

$$\begin{aligned}\partial_t a &= \nu\partial_r^2 a + \mathfrak{z}_1\partial_r a + \mathfrak{z}_2\partial_r b + \partial_r \eta^- \\ \partial_t b &= \nu\partial_r^2 b + \mathfrak{z}_1\partial_r b - \mathfrak{z}_2\partial_r a - \partial_r \eta^+\end{aligned}$$

Only if one chooses $\mathfrak{z}_1 = 0$, one obtains an oscillatory equation $\nu^2 p'' = -\mathfrak{z}_{2,\infty}^2 p$ for the derivative $p := \lim_{t \rightarrow \infty} \partial_r \langle a \rangle$ of the noise-averaged stationary slope, and similarly for $q := \lim_{t \rightarrow \infty} \partial_r \langle b \rangle$. The effect of this formally ‘imaginary’ Lagrange multiplier is included in the equations of motion (2.3).

Conservation laws become explicit by rewriting the complex equations of motion (1.5)

$$\begin{aligned}\partial_t(a + ib) &= \partial_r^2(a + ib) + \mathfrak{z}(t)\partial_r(a + ib) + \partial_r(\eta^- - i\eta^+) \\ &= \partial_r [(\partial_r - i\mathfrak{z}(t))(a + ib) - i(\eta^+ + i\eta^-)]\end{aligned}$$

in the form of a continuity equation. Using $u = a + ib$ and its formal complex conjugate $u^* = a - ib$, along with $\zeta := \eta^+ + i\eta^-$ and $\zeta^* = \eta^+ - i\eta^-$, we have the pair of equations

$$\partial_t u = \partial_r [(\partial_r - i\mathfrak{z}(t))u - i\zeta] \quad , \quad \partial_t u^* = \partial_r [(\partial_r + i\mathfrak{z}(t))u^* + i\zeta^*] \quad (2.8)$$

and identify the densities $j = (\partial_r - i\mathfrak{z}(t))u - i\zeta$ and $j^* = (\partial_r + i\mathfrak{z}(t))u^* + i\zeta^*$ of the conserved currents, such that the ‘conserved charges’ $U = \int_{\mathbb{R}} dr u(t, r)$ and $U^* = \int_{\mathbb{R}} dr u^*(t, r)$ are time-independent, viz. $\partial_t U = \partial_t U^* = 0$.

2.3 Definition of the third Arcetri model

Analogously, for the third Arcetri model we start from the height profile $h(t, r)$, decomposed into even and odd parts

$$h(t, r) = a(t, r) + b(t, r) \quad (2.9)$$

and write down the defining equations of motion (on a discrete chain of N sites)

$$\partial_t a_n(t) = \nu (a_{n+1}(t) + a_{n-1}(t) - 2a_n(t)) + \frac{1}{2} \mathfrak{z}(t) (b_{n+1}(t) - b_{n-1}(t)) + \eta_n^+(t) \quad (2.10)$$

$$\partial_t b_n(t) = \nu (b_{n+1}(t) + b_{n-1}(t) - 2b_n(t)) - \frac{1}{2} \mathfrak{z}(t) (a_{n+1}(t) - a_{n-1}(t)) + \eta_n^-(t)$$

with the symmetrised noise (2.5). In this physical context, it appears natural to use initially uncorrelated gaussian slopes

$$\begin{aligned} \langle\langle a_n(0) \rangle\rangle &= H_0 \quad , \quad \langle\langle b_n(0) \rangle\rangle = 0 \quad , \quad \langle\langle a_n(0) b_m(0) \rangle\rangle = 0 \\ \langle\langle a_n(0) a_m(0) \rangle\rangle_c &= \frac{1}{2} H_1 (\delta_{n,m} + \delta_{n,N-m}) \quad , \quad \langle\langle b_n(0) b_m(0) \rangle\rangle = \frac{1}{2} H_1 (\delta_{n,m} - \delta_{n,N-m}) \end{aligned} \quad (2.11)$$

The Lagrange multiplier $\mathfrak{z}(t)$ is found from the mean spherical constraint on the slopes

$$\left\langle\left\langle \sum_{n=1}^N (\nabla a_n(t) + \nabla b_n(t))^2 \right\rangle\right\rangle = N \quad (2.12)$$

where $\nabla f_n = \frac{1}{2} (f_{n+1} - f_{n-1})$ is the symmetrised spatial difference. The initial conditions (2.11) are natural for an interpretation of $h(t, r)$ as the height of a growing and fluctuating interface, which is flat on average.

Eqs. (2.10,2.11,2.12), together with the noise correlator (2.5), define the **third Arcetri model**.

Formally, one might obtain this from the modified KPZ equation (1.6) by introducing a complex height $h = a + ib$, a complex Lagrange multiplier $\mathfrak{z}(t) = \mathfrak{z}_1(t) - i\mathfrak{z}_2(t)$ and a complex noise $\eta(t, r) = \eta^+(t, r) + i\eta^-(t, r)$. As before, only if one chooses $\mathfrak{z}_1 = 0$, the derivative $p := \lim_{t \rightarrow \infty} \partial_r \langle a \rangle$ of the stationary height obeys an oscillatory equation $\nu^2 p'' = -\mathfrak{z}_{2,\infty}^2 p$. Because of the ‘non-conserved’ noise, there are no obvious conservation laws, for $T \neq 0$.

All definitions were only made explicit in $d = 1$ spatial dimensions. Eventual extensions to $d > 1$ are left for future work.

3 Solution

We begin our discussion with the second Arcetri model. The treatment of the third Arcetri model being fairly analogous, we shall simply quote the relevant results in section 3.4.

3.1 Second model: General form

The first step to the solution of eqs. (2.3) proceeds via Fourier-transform, but we must take into account the specific parity of the a_n and b_n . Therefore, we use the representation in terms of discrete cosine- and sine-transforms,

$$a_n(t) = \frac{1}{N} \sum_{k=0}^{N-1} \cos\left(\frac{2\pi}{N}kn\right) \hat{a}(t, k) \quad , \quad b_n(t) = \frac{1}{N} \sum_{k=0}^{N-1} \sin\left(\frac{2\pi}{N}kn\right) \hat{b}(t, k) \quad (3.1)$$

see appendix F for details. Using eqs. (F.3,F.4,F.5,F.6), the equations of motion turn into

$$\begin{aligned} \partial_t \hat{a}(t, k) &= -2\nu \left(1 - \cos\left(\frac{2\pi}{N}k\right)\right) \hat{a}(t, k) + \mathfrak{z}(t) \sin\left(\frac{2\pi}{N}k\right) \hat{b}(t, k) + \sin\left(\frac{2\pi}{N}k\right) \hat{\eta}^-(t, k) \\ \partial_t \hat{b}(t, k) &= -2\nu \left(1 - \cos\left(\frac{2\pi}{N}k\right)\right) \hat{b}(t, k) + \mathfrak{z}(t) \sin\left(\frac{2\pi}{N}k\right) \hat{a}(t, k) + \sin\left(\frac{2\pi}{N}k\right) \hat{\eta}^+(t, k) \end{aligned} \quad (3.2)$$

Although we shall use the same notation for both cosine- and sine-transforms, the parity must be taken into account for the inverse transformation. We shall use the short-hands

$$\omega(k) := 1 - \cos\left(\frac{2\pi}{N}k\right) \quad , \quad \lambda(k) := \sin\left(\frac{2\pi}{N}k\right) \quad , \quad Z(t) := \int_0^t d\tau \mathfrak{z}(\tau) \quad (3.3)$$

Later, when taking the continuum limit, it will be enough to simply replace $\omega(k) \rightarrow 1 - \cos k$ and $\lambda(k) \rightarrow \sin k$, and to consider $k \in (-\pi, \pi)$ instead of $k = 0, 1, \dots, N-1$ on the chain.

The above equations (3.2) are decoupled by going over to the combinations $\hat{f}_{\pm}(t, k) := \hat{a}(t, k) \pm \hat{b}(t, k)$, which obey the equations

$$\partial_t \hat{f}_{\pm}(t, k) = (-2\nu\omega(k) \pm \lambda(k)\mathfrak{z}(t)) \hat{f}_{\pm}(t, k) + \lambda(k) (\hat{\eta}^-(t, k) \pm \hat{\eta}^+(t, k)) \quad (3.4)$$

with the solutions

$$\begin{aligned} \hat{f}_{\pm}(t, k) &= \hat{f}_{\pm,00}(k) \exp[-2\nu\omega(k)t \pm \lambda(k)Z(t)] \\ &+ \int_0^t d\tau \lambda(k) (\hat{\eta}^-(\tau, k) \pm \hat{\eta}^+(\tau, k)) \exp[-2\nu\omega(k)(t-\tau) \pm \lambda(k)(Z(t)-Z(\tau))] \end{aligned} \quad (3.5)$$

and where the functions $\hat{f}_{\pm,00}$ are to be found from the initial conditions. Going back to the parity eigenstates, using that $\hat{a} = \frac{1}{2}(\hat{f}_+ + \hat{f}_-)$ and $\hat{b} = \frac{1}{2}(\hat{f}_+ - \hat{f}_-)$, we have explicitly

$$\begin{aligned} \hat{a}(t, k) &= \frac{1}{2} \left[\hat{f}_{+,00}(k) e^{-2\nu\omega(k)t + \lambda(k)Z(t)} + \hat{f}_{-,00}(k) e^{-2\nu\omega(k)t - \lambda(k)Z(t)} \right] \\ &+ \frac{1}{2} \int_0^t d\tau \lambda(k) \left[(\hat{\eta}^-(\tau, k) + \hat{\eta}^+(\tau, k)) e^{-2\nu\omega(k)(t-\tau) + \lambda(k)(Z(t)-Z(\tau))} \right. \\ &\quad \left. + (\hat{\eta}^-(\tau, k) - \hat{\eta}^+(\tau, k)) e^{-2\nu\omega(k)(t-\tau) - \lambda(k)(Z(t)-Z(\tau))} \right] \end{aligned} \quad (3.6)$$

$$\begin{aligned} \hat{b}(t, k) &= \frac{1}{2} \left[\hat{f}_{+,00}(k) e^{-2\nu\omega(k)t + \lambda(k)Z(t)} - \hat{f}_{-,00}(k) e^{-2\nu\omega(k)t - \lambda(k)Z(t)} \right] \\ &+ \frac{1}{2} \int_0^t d\tau \lambda(k) \left[(\hat{\eta}^-(\tau, k) + \hat{\eta}^+(\tau, k)) e^{-2\nu\omega(k)(t-\tau) + \lambda(k)(Z(t)-Z(\tau))} \right. \\ &\quad \left. - (\hat{\eta}^-(\tau, k) - \hat{\eta}^+(\tau, k)) e^{-2\nu\omega(k)(t-\tau) - \lambda(k)(Z(t)-Z(\tau))} \right] \end{aligned} \quad (3.7)$$

and a cosine or sine transformation, respectively, will bring back $a_n(t)$ and $b_n(t)$. For the chosen initial conditions, we simply have $\langle\langle \hat{a}(t, k) \rangle\rangle = \langle\langle \hat{b}(t, k) \rangle\rangle = 0$ which implies in turn $\langle\langle a_n(t) \rangle\rangle = \langle\langle b_n(t) \rangle\rangle = 0$, that is, the interface is always flat on average.

3.2 Second model: spherical constraint

The next step in the solution of the model consists of casting the spherical constraint into an equation for $Z(t)$. To do so, the constraint (2.7) is rewritten in Fourier space

$$\left\langle\left\langle\sum_{n=1}^N (a_n(t) + b_n(t))^2\right\rangle\right\rangle = \frac{1}{N} \left\langle\left\langle\sum_{k=0}^{N-1} [\hat{a}(t, k)\hat{a}(t, k) + \hat{b}(t, k)\hat{b}(t, k)]\right\rangle\right\rangle = N \quad (3.8)$$

Initial conditions must be such that the spherical constraint is respected at $t = 0$, hence

$$\frac{1}{N} \left\langle\left\langle\sum_{k=0}^{N-1} [\hat{a}(0, k)\hat{a}(0, k) + \hat{b}(0, k)\hat{b}(0, k)]\right\rangle\right\rangle = \frac{1}{2N} \left\langle\left\langle\sum_{k=0}^{N-1} f_{+,00}^2(k) + f_{-,00}^2(k)\right\rangle\right\rangle = N \quad (3.9)$$

where the solution (3.6,3.7) was used. From the initial conditions (2.6) of initially uncorrelated slopes, we have

$$\left\langle\left\langle\hat{f}_{\pm,00}(k)\right\rangle\right\rangle = 0 \quad , \quad \left\langle\left\langle\hat{f}_{\pm,00}(k)^2\right\rangle\right\rangle = N \quad , \quad \left\langle\left\langle\hat{f}_{+,00}(k)\hat{f}_{-,00}(k')\right\rangle\right\rangle = 0 \quad (3.10)$$

The non-vanishing noise correlators read in Fourier space

$$\langle\hat{\eta}^{\pm}(t, k)\hat{\eta}^{\pm}(t', k')\rangle = N\nu T\delta(t - t') [\delta_{k+k',0} \pm \delta_{k-k',0}] \quad (3.11)$$

such that the constraint can be reexpressed as follows, for this kind of initial condition

$$1 = \frac{1}{2N} \sum_{k=0}^{N-1} \left\{ \left[e^{2\lambda(k)Z(t)} + e^{-2\lambda(k)Z(t)} \right] e^{-4\nu\omega(k)t} + 2\nu T\lambda^2(k) \int_0^t d\tau e^{-4\nu\omega(k)(t-\tau)} \left[e^{2\lambda(k)(Z(t)-Z(\tau))} + e^{-2\lambda(k)(Z(t)-Z(\tau))} \right] \right\} \quad (3.12)$$

The asymptotic analysis of this equation is greatly simplified in the continuum limit, when it takes the form

$$\int_0^\pi dk \left[\cosh(2\lambda(k)Z(t)) e^{-4\nu\omega(k)t} + 2\nu T\lambda^2(k) \int_0^t d\tau \cosh(2\lambda(k)(Z(t) - Z(\tau))) e^{-4\nu\omega(k)(t-\tau)} \right] = \pi \quad (3.13)$$

where the auxiliary functions (3.3) now stand for their continuum versions $\omega(k) = 1 - \cos k$ and $\lambda(k) = \sin k$.

In what follows, we shall require the following identities, with $a \in \mathbb{N}$

$$\begin{aligned} \mathcal{J}_{2a}(A, Z) &:= \frac{1}{\pi} \int_0^\pi dk e^{A \cos k} \cosh(Z \sin k) (\sin k)^{2a} = \frac{\partial^{2a} \mathcal{J}_0(A, Z)}{\partial Z^{2a}} = \frac{\partial^{2a} I_0(\sqrt{A^2 + Z^2})}{\partial Z^{2a}} \\ \mathcal{J}_{2a+1}(A, Z) &:= \frac{1}{\pi} \int_0^\pi dk e^{A \cos k} \sinh(Z \sin k) (\sin k)^{2a+1} = \frac{\partial^{2a+1} I_0(\sqrt{A^2 + Z^2})}{\partial Z^{2a+1}} \end{aligned} \quad (3.14)$$

which are proven in appendix D and where I_0 is a modified Bessel function [1]. The constraint (3.13) can be written more compactly as follows

$$e^{-4\nu t} \mathcal{J}_0(4\nu t, 2Z(t)) + 2\nu T \int_0^t d\tau e^{-4\nu(t-\tau)} \mathcal{J}_2(4\nu(t-\tau), 2Z(t) - 2Z(\tau)) = 1 \quad (3.15)$$

In contrast to the first Arcetri model [39], or well-known kinetic spherical models [67, 19, 29], this equation does not take the form of an easily-solved Volterra integral equation.

3.3 Second model: observables

The observables we are interested in are the two-time correlation and response functions and shall be defined carefully.

For the correlation function, as the order parameter is the local slope $u_n(t)$, one might expect that $\langle u_n(t)u_m(s) \rangle$ should describe the two-time temporal-spatial correlator $C_{n,m}(t, s)$. However, a physically sensible definition of correlators must obey two symmetry conditions: first, for equal times, the purely spatial correlator $C_{n,m}(t, t) = C_{m,n}(t, t)$ and second, the two-time autocorrelator $C_{n,n}(t, s) = C_{n,n}(s, t)$ are both symmetric. Therefore, we recall the decomposition $u_n(t) = a_n(t) + b_n(t)$ into an even and an odd part and adopt the definition⁸

$$C_{n,m}(t, s) := \langle\langle a_n(t)a_m(s) \rangle\rangle + \langle\langle b_n(t)b_m(s) \rangle\rangle \quad (3.16)$$

Now, using (3.6,3.7) together with the cosine and sine transforms, we find

$$\begin{aligned} C_{n,m}(t, s) = & \frac{1}{N} \sum_{k=0}^{N-1} \cos\left(\frac{2\pi}{N}k(n-m)\right) \left[e^{-2\nu\omega(k)(t+s)} \cosh(\lambda(k)(Z(t) + Z(s))) \right. \\ & \left. + 2\nu T \int_0^{\min(t,s)} d\tau \lambda^2(k) e^{-2\nu\omega(k)(t+s-2\tau)} \cosh(\lambda(k)(Z(t) + Z(s) - 2Z(\tau))) \right] \end{aligned} \quad (3.17)$$

which in the continuum limit $N \rightarrow \infty$ becomes, where n, m are still considered as integers

$$\begin{aligned} C_{n,m}(t, s) = & \frac{1}{2\pi} \int_{-\pi}^{\pi} \cos(k(n-m)) \left[e^{-2\nu(1-\cos(k))(t+s)} \cosh(\sin(k)(Z(t) + Z(s))) \right. \\ & \left. + 2\nu T \int_0^{\min(t,s)} d\tau \sin^2(k) e^{-2\nu(1-\cos(k))(t+s-2\tau)} \cosh(\sin(k)(Z(t) + Z(s) - 2Z(\tau))) \right]. \end{aligned} \quad (3.18)$$

The requested symmetries, mentioned above, are now obvious. Furthermore, spatial translation-invariance is now manifest and we can write $C_{n,m}(t, s) = C_{n-m}(t, s)$. A more explicit form is obtained by using the identity, valid for $n \in \mathbb{N}$ and $A, Z \in \mathbb{C}$

$$\mathcal{C}_n(A, Z) := \frac{1}{\pi} \int_0^\pi dk e^{A \cos k} \cosh(Z \sin k) \cos(nk) = I_n\left(\sqrt{A^2 + Z^2}\right) \cos\left(n \arctan\left(\frac{Z}{A}\right)\right) \quad (3.19)$$

which is proven in appendix E. This gives, where for notational simplicity we let $t > s$

$$\begin{aligned} C_n(t, s) = & e^{-2\nu(t+s)} \mathcal{C}_n(2\nu(t+s), Z(t) + Z(s)) \\ & + 2\nu T \int_0^s d\tau e^{-2\nu(t+s-2\tau)} \frac{\partial^2}{\partial Z(t) \partial Z(s)} \mathcal{C}_n(2\nu(t+s-2\tau), Z(t) + Z(s) - 2Z(\tau)) \end{aligned} \quad (3.20)$$

In this work, we shall concentrate on the case $T = 0$. Then, with (3.19), the two-time slope correlator reads explicitly, in terms of the integrated Lagrange multiplier $Z(t)$

$$\begin{aligned} C_n(t, s) = & e^{-2\nu(t+s)} \mathcal{C}_n(2\nu(t+s), Z(t) + Z(s)) \\ = & e^{-2\nu(t+s)} I_n\left(\sqrt{(2\nu(t+s))^2 + (Z(t) + Z(s))^2}\right) \cos\left(n \arctan\left(\frac{Z(t) + Z(s)}{2\nu(t+s)}\right)\right) \end{aligned} \quad (3.21)$$

⁸If we were to consider a complex-valued solution $u_n(t) = a_n(t) + ib_n(t)$ of the Burgers equation, see section 2, the definition (3.16) would correspond to $\langle u_n(t)u_m(s)^* \rangle$.

and we shall extract its long-time scaling behaviour in the next section, after having found $Z(t)$ from (3.15). Remarkably, in the large-time limit $t, s \rightarrow \infty$, we shall see that the time-space behaviour simplifies in the sense that the leading term of the correlator

$$C_n(t, s) \simeq C(t, s) \exp \left(-\frac{n^2}{4\nu(t+s)} \right) \cos \left(n \arctan \left(\frac{Z(t) + Z(s)}{2\nu(t+s)} \right) \right) \quad (3.22)$$

factorises into the autocorrelator $C(t, s) = C_0(t, s)$ and a second factor, which alone determines the spatial behaviour.

In order to define the linear response of the order-parameter, here identified with the local slope, a choice of the external perturbation must be made. Here, we consider the effect of a small perturbation $j_n(t)$, of the slope, on the slope itself. In generalising the equations of motion, the external perturbation must be decomposed in the even and odd parts $j_n^\pm(t)$, respectively

$$\begin{aligned} \partial_t a_n(t) &= \nu (a_{n+1}(t) + a_{n-1}(t) - 2a_n(t)) + \frac{\mathfrak{z}(t)}{2} (b_{n+1}(t) - b_{n-1}(t)) \\ &\quad + \frac{1}{2} (\eta_{n+1}^-(t) - \eta_{n-1}^-(t)) + j_n^+(t) \end{aligned} \quad (3.23)$$

$$\begin{aligned} \partial_t b_n(t) &= \nu (b_{n+1}(t) + b_{n-1}(t) - 2b_n(t)) - \frac{\mathfrak{z}(t)}{2} (a_{n+1}(t) - a_{n-1}(t)) \\ &\quad - \frac{1}{2} (\eta_{n+1}^+(t) - \eta_{n-1}^+(t)) + j_n^-(t) \end{aligned} \quad (3.24)$$

where $j_n^+(t)$ and $j_n^-(t)$, respectively, are the conjugate fields associated with the even and odd parts of the order-parameter $a_n(t)$ and $b_n(t)$. The solution of these equations follows the same lines which have led to (3.6,3.7), with the replacements $\lambda(k)\hat{\eta}^\pm \mapsto \lambda(k)\hat{\eta}^\pm + \hat{j}^\mp$.

The response function is defined as

$$R_{n,m}(t, s) := \left\langle \left\langle \frac{\delta a_n(t)}{\delta j_m^+(s)} \right|_{j=0} \right\rangle \right\rangle + \left\langle \left\langle \frac{\delta b_n(t)}{\delta j_m^-(s)} \right|_{j=0} \right\rangle \right\rangle \quad (3.25)$$

and clearly, only the average over the initial condition (2.6) needs to be taken, the thermal average becoming trivial. This also implies that the temperature T does not enter explicitly into the response function. Inserting the explicit solution, we readily find, also writing the causality condition $t > s$ through the Heaviside function Θ

$$\begin{aligned} R_{n,m}(t, s) &= \frac{\Theta(t-s)}{N} \int_0^t d\tau \sum_{k,\ell=0}^{N-1} e^{2\nu\omega(k)(t-\tau)} \cosh \left(\lambda(k) (Z(t) - Z(\tau)) \right) \\ &\quad \times \left[\cos \left(\frac{2\pi}{N} kn \right) \cos \left(\frac{2\pi}{N} k\ell \right) + \sin \left(\frac{2\pi}{N} kn \right) \sin \left(\frac{2\pi}{N} k\ell \right) \right] \delta(\tau - s) \delta_{\ell,m} \\ &= \frac{\Theta(t-s)}{N} \sum_{k=0}^{N-1} e^{2\nu\omega(k)(t-s)} \cosh \left(\lambda(k) (Z(t) - Z(s)) \right) \cos \left(\frac{2\pi}{N} k(n-m) \right) \end{aligned} \quad (3.26)$$

which is spatially translation-invariant, as it should be, hence $R_{n,m}(t, s) = R_{n-m}(t, s)$. In the $N \rightarrow \infty$ limit, this simplifies into, using (3.19)

$$\begin{aligned} R_n(t, s) &= \frac{\Theta(t-s)}{\pi} \int_0^\pi dk e^{-2\nu(1-\cos k)(t-s)} \cosh \left((Z(t) - Z(s)) \sin k \right) \cos kn \\ &= \Theta(t-s) e^{-2\nu(t-s)} I_n \left(\sqrt{4\nu^2(t-s)^2 + (Z(t) - Z(s))^2} \right) \cos \left(n \arctan \left(\frac{Z(t) - Z(s)}{2\nu(t-s)} \right) \right) \end{aligned} \quad (3.27)$$

In the next section, using (3.15), the asymptotic long-time scaling behaviour will be analysed. Again, we find that for large times, the leading term simplifies

$$R_n(t, s) \simeq R(t, s) \exp \left(-\frac{n^2}{4\nu(t-s)} \right) \cos \left(n \arctan \left(\frac{Z(t) - Z(s)}{2\nu(t-s)} \right) \right) \quad (3.28)$$

into a product of the autoresponse $R(t, s) = R_0(t, s)$ and a second factor, which determines the spatial dependence alone.

Alternatively, one might also consider how the local slope will respond to a small change in the height variable. In this case, it is enough to replace $\eta \mapsto \eta + j$ in the equations of motion (2.3). The formal definition of the response function is still given by (3.25), although the physical meaning of the external fields $j_n^\pm(t)$ has changed. The explicit calculation is analogous to the previous ones and we just quote the result

$$\begin{aligned} \mathcal{R}_n(t, s) &= \frac{\Theta(t-s)}{N} \sum_{k=0}^{N-1} \lambda(k) e^{-2\nu\omega(k)(t-s)} \sinh \left(\lambda(k) (Z(t) - Z(s)) \right) \cos \left(\frac{2\pi}{N} kn \right) \\ &\stackrel{N \rightarrow \infty}{=} \frac{\Theta(t-s)}{\pi} \int_0^\pi dk e^{-2\nu(1-\cos k)(t-s)} \sinh \left((Z(t) - Z(s)) \sin k \right) \sin(k) \cos(kn) \\ &= \Theta(t-s) e^{-2\nu(t-s)} \times \\ &\quad \times \frac{\partial}{\partial Z(t)} \left[I_n \left(\sqrt{4\nu^2(t-s)^2 + (Z(t) - Z(s))^2} \right) \cos \left(n \arctan \left(\frac{Z(t) - Z(s)}{2\nu(t-s)} \right) \right) \right] \end{aligned} \quad (3.29)$$

where we have used (3.19) again. The asymptotic behaviour follows from the one of $Z(t)$.

3.4 Third model

In order to define the observables of the third Arcetri model, re-write first the (anti-)symmetrised equations of motion in Fourier space

$$\begin{aligned} \partial_t \hat{a}(t, k) &= -2\nu\omega(k) \hat{a}(t, k) + \mathfrak{z}(t) \lambda(k) \hat{b}(t, k) + \hat{\eta}^+(t, k) \\ \partial_t \hat{b}(t, k) &= -2\nu\omega(k) \hat{b}(t, k) + \mathfrak{z}(t) \lambda(k) \hat{a}(t, k) + \hat{\eta}^-(t, k) \end{aligned} \quad (3.30)$$

where we used the abbreviations (3.3). The solution of these equations reads

$$\begin{aligned} \left. \begin{array}{l} \hat{a}(t, k) \\ \hat{b}(t, k) \end{array} \right\} &= \frac{1}{2} \left[\hat{f}_{+,00}(k) e^{-2\nu\omega(k)t + \lambda(k)Z(t)} \pm \hat{f}_{-,00}(k) e^{-2\nu\omega(k)t - \lambda(k)Z(t)} \right] \\ &\quad + \frac{1}{2} \int_0^t d\tau \left[(\hat{\eta}^+(\tau, k) + \hat{\eta}^-(\tau, k)) e^{-2\nu\omega(k)(t-\tau) + \lambda(k)(Z(t)-Z(\tau))} \right. \\ &\quad \left. \pm (\hat{\eta}^+(\tau, k) - \hat{\eta}^-(\tau, k)) e^{-2\nu\omega(k)(t-\tau) - \lambda(k)(Z(t)-Z(\tau))} \right] \end{aligned} \quad (3.31)$$

where the upper signs correspond to \hat{a} and the lower signs to \hat{b} . The spherical constraint is now give by eq. (2.12) and takes the form

$$\frac{1}{N} \left\langle \left\langle \sum_{k=0}^{N-1} \left[\lambda(k)^2 \left[\hat{a}(t, k) \hat{a}(t, k) + \hat{b}(t, k) \hat{b}(t, k) \right] \right] \right\rangle \right\rangle = N \quad (3.32)$$

This can be evaluated along the same lines as before. We merely quote the end result, in the continuum limit

$$e^{-4\nu t} \mathcal{J}_2(4\nu t, 2Z(t)) + 2\nu T \int_0^t d\tau e^{-4\nu(t-\tau)} \mathcal{J}_2(4\nu(t-\tau), 2Z(t) - 2Z(\tau)) = 1 \quad (3.33)$$

If $T = 0$, the conservation laws (2.8) obtained for the second model also hold for the third. This implies a constant height profile $\langle\langle h(t, r) \rangle\rangle = H_0$, where for simplicity, we used the initial conditions (2.11). From now on, we set $H_0 = 0$ in (2.11), without restriction to the generality.

The time-space correlator is defined analogously as in the second model, by eq. (3.16), but now using the decomposition $h_n(t) = a_n(t) + b_n(t)$ of the height in an even and an odd part. Although we re-use the formal definition eq. (3.16), the physical interpretation is now a different one and gives a height-height correlator. The main computational difference with respect to the second model is the absence of the factor $\lambda(k)$ before the thermal noise $\hat{\eta}^\pm$. For the initial conditions (2.11), spatial translation-invariance holds for all times $t, s > 0$, so that we can write $C_{n-m}(t, s) = C_{n,m}(t, s)$. We finally have, using (3.15)

$$\begin{aligned} C_n(t, s) &= e^{-2\nu(t+s)} \mathcal{C}_n(2\nu(t+s), Z(t) + Z(s)) \\ &\quad + 2\nu T \int_0^{\min(t,s)} d\tau e^{-2\nu(t+s-2\tau)} \mathcal{C}_n(2\nu(t+s-2\tau), Z(t) + Z(s) - 2Z(\tau)) \end{aligned} \quad (3.34)$$

In particular, for $T = 0$, we recover the same abstract expression, eq. (3.21), as for the slope-slope correlator $C_n^{(II)}(t, s)$ but with the difference that $Z(t)$ now has to be found from the spherical constraint (3.33).

For the calculation of the linear response of the height with respect to a small change in the height, one replaces $\hat{\eta}^\pm \mapsto \hat{\eta}^\pm + \hat{j}^\pm$ in the equation of motion (3.31). We can simply re-use the definition (3.25), and formally recover the abstract form

$$\begin{aligned} R_n(t, s) &= \Theta(t-s) e^{-2\nu(t-s)} \times \\ &\quad \times I_n \left(\sqrt{4\nu^2(t-s)^2 + (Z(t) - Z(s))^2} \right) \cos \left(n \arctan \left(\frac{Z(t) - Z(s)}{2\nu(t-s)} \right) \right) \end{aligned} \quad (3.35)$$

identical to (3.27). In particular, in the long-times limit and for $T = 0$, both the height correlator and the height response factorise, as in (3.22, 3.28), respectively. Again, $Z(t)$ is found from (3.33).

4 Long-time behaviour

4.1 Spherical constraint at $T = 0$

First, we have to determine the long-time behaviour of the Lagrange multiplier $Z(t)$, from the spherical constraints eqs. (3.15, 3.33). From now on, we shall restrict to the case $T = 0$.

For the second model, eq. (3.15) reduces to

$$e^{-4\nu t} I_0 \left(4\nu t \sqrt{1 + \left(\frac{Z(t)}{2\nu t} \right)^2} \right) = 1. \quad (4.1)$$

In appendix B, we shall show that for large times $Z(t) \simeq \sqrt{\nu t \ln(8\pi\nu t)}$.

For the third model, we must solve eq. (3.33). In appendix B it is shown that this is equivalent to

$$\begin{aligned} & \left[I_1 \left(\sqrt{(4\nu t)^2 + (2Z(t))^2} \right) (4\nu t)^2 \right. \\ & \left. + 2Z(t)^2 \sqrt{(4\nu t)^2 + (2Z(t))^2} \left(I_0 \left(\sqrt{(4\nu t)^2 + (2Z(t))^2} \right) + I_2 \left(\sqrt{(4\nu t)^2 + (2Z(t))^2} \right) \right) \right] \\ & = e^{4\nu t} [(4\nu t)^2 + (2Z(t))^2]^{-3/2} \end{aligned} \quad (4.2)$$

To leading order, this would give the solution $Z(t) \simeq \sqrt{3\nu t \ln((32\pi e)^{1/3} \nu t)}$. Then, this could be combined with the second model as follows: for t large enough, we have

$$Z(t) = \sqrt{\kappa_1 \nu t \ln(\kappa_2 t)} \quad , \quad \begin{cases} \kappa_1 = 1 & , & \kappa_2 = 8\pi\nu & \text{second model} \\ \kappa_1 = 3 & , & \kappa_2 = (32\pi e)^{1/3}\nu & \text{third model} \end{cases} \quad (4.3)$$

However, as also shown in appendix B, it is advisable to include the next-to-leading terms as well. If that is done, we find, for the third model and t large enough

$$Z(t) \simeq \sqrt{2tW\left((32\pi e)^{1/2} t^{3/2}\right)} - t \simeq \sqrt{3t \ln(\kappa_2 t) \left[1 - \frac{2 \ln(\frac{3}{2} \ln \kappa_2 t)}{3 \ln \kappa_2 t} - \frac{1}{3 \ln \kappa_2 t} \right]} \quad (4.4)$$

where $W(x)$ denotes Lambert's W -function [55, 16]. The results (4.3), and (4.4) for the third model, are the basis of the entire asymptotic analysis. Formally, for truly enormous times $t \gg 1$, the distinction between the second and the third model merely comes from the values of the two constants $\kappa_{1,2}$, as given in (4.3), and both models can be analysed together. However, the further logarithmic corrections in (4.4) will lead to some significant differences between the second and the third model, even for $T = 0$, as we shall now see. In the main text, we merely quote our results and refer to appendices B and C for the calculations.

4.2 Zero-temperature correlators

We now turn to the correlators. For a vanishing temperature $T = 0$, we have already shown in (3.21,3.22) that the time-space correlator $C_n(t, s)$ factorises into the autocorrelator $C(t, s)$ and a space-dependent part. The autocorrelator takes the form

$$C(t, s) = e^{-2\nu(t+s)} I_0 \left(2\nu(t+s) \sqrt{1 + \left(\frac{Z(t) + Z(s)}{2\nu(t+s)} \right)^2} \right) \quad (4.5)$$

where $Z(t)$ is given by (4.3). This autocorrelator does *not* obey the scaling of simple ageing, where $t, s \rightarrow \infty$ and $y = t/s > 1$ is kept fixed. We rather must consider a different scaling behaviour, where again $t, s \rightarrow \infty$ such that a certain scaling variable y is being kept fixed. We find two possibilities:

1. the time difference is given by⁹

$$\tau = t - s = (y - 1) \frac{s}{\ln^{1/2} \kappa_2 s}. \quad (4.6)$$

⁹The notation is chosen such that one returns to simple ageing, if the logarithmic factors are dropped.

and we have the scaling form

$$C(t, s) = C^{(0)} (\ln s)^{(\kappa_1 - 1 - \delta_{\kappa_1, 3})/2} \exp \left(-\frac{\kappa_1}{32} (y - 1)^2 \right) \quad (4.7)$$

with the constant $C^{(0)} = \sqrt{\kappa_2^{\kappa_1}/(8\pi\nu)}$ for the second model and $C^{(0)} = \sqrt{\kappa_2^{\kappa_1} e^{1/2}/(12\pi\nu)}$ for the third model. The scaling (4.6, 4.7) was seen before in the phase-separation kinetics of the spherical model, at temperature $T = 0$, with a conserved order parameter (model B dynamics) [9].

2. the time difference is given by, with $\vartheta > \frac{1}{2}$

$$\tau = t - s = \frac{s}{\ln^{1/2}(\kappa_2 s)} \sqrt{W((y - 1)^2 \ln^{1-2\vartheta}(\kappa_2 s))} \quad (4.8)$$

where $W(x)$ is, again, Lambert's W -function. For $s \rightarrow \infty$, this gives $\tau \simeq (y - 1)s \ln^{-\vartheta}(\kappa_2 s)$. The autocorrelator becomes

$$C(t, s) = C^{(0)} (\ln(\kappa_2 s))^{(\kappa_1 - 1 - \delta_{\kappa_1, 3})/2} \quad (4.9)$$

As we shall see, we must further distinguish here the cases $\frac{1}{2} < \vartheta < 1$ and $\vartheta > 1$.

A scaling behaviour according to (4.6, 4.8) corresponds to *logarithmic sub-ageing*, since the time difference $\tau = t - s$ grows more slowly than s , by a logarithmic factor.¹⁰ Although the forms (4.6, 4.8) are distinct from simple ageing as described in section 1, we shall cast the autocorrelator into a scaling form $C(t, s) = s^{-b} \ln^{-\hat{b}} s f_C(y)$ and shall check for an asymptotic form $f_C(y) \sim y^{-\lambda_C/z} \ln^{\hat{\lambda}_C/z} s$ as $y \rightarrow \infty$. If these forms apply, the exponents b , λ_C are quoted in tables 1 and 2. By analogy with equilibrium critical phenomena, we also introduce the *logarithmic sub-scaling exponents* \hat{b} , $\hat{\lambda}_C$ [50]. We find $\hat{b} = \hat{\lambda}_C = 0$ for the second Arcetri model and $\hat{b} = -\frac{1}{2}$, $\hat{\lambda}_C = 0$ for the third Arcetri model.

Concerning the equal-time autocorrelator $C(t, t) = (\ln(\kappa_2 t))^{(\kappa_1 - 1 - \delta_{\kappa_1, 3})/2}$ in both scaling regimes, there is a difference in interpretation between the second and the third model. In the second model, $C(t, t) = 1$ because of the constraint (4.1), which is consistent with a probabilistic interpretation, either in terms of the slopes or else in terms of particles and holes. Indeed, one has $\kappa_1 = 1$ in this case. For the third model, $C(t, t) = w^2(t) = (\ln \kappa_2 t)^{1/2}$ is simply the square of the interface width $w(t) \sim t^\beta \ln^{\hat{\beta}} t$. Hence for $d = 1$, where $\kappa_1 = 3$, the interface is logarithmically rough, with growth exponents $\beta = 0$ and $\hat{\beta} = \frac{1}{4}$.

The time-space-dependent slope-slope correlator $C_n(t, s)$ is given by (3.22). This yields the following long-time behaviour

$$C_n(t, s) \simeq C(t, s) \exp \left(-\frac{1}{2} \left(\frac{n}{\sqrt{2\nu(t+s)}} \right)^2 \right) \cos \left(\frac{n}{\sqrt{2\nu(t+s)}} \sqrt{\frac{\kappa_1}{2} (\ln \kappa_2 t + \ln \kappa_2 s)} \right) \quad (4.10)$$

¹⁰Simple inequalities exclude the opposite case of ‘super-ageing’ where $t - s$ would grow faster than s [54].

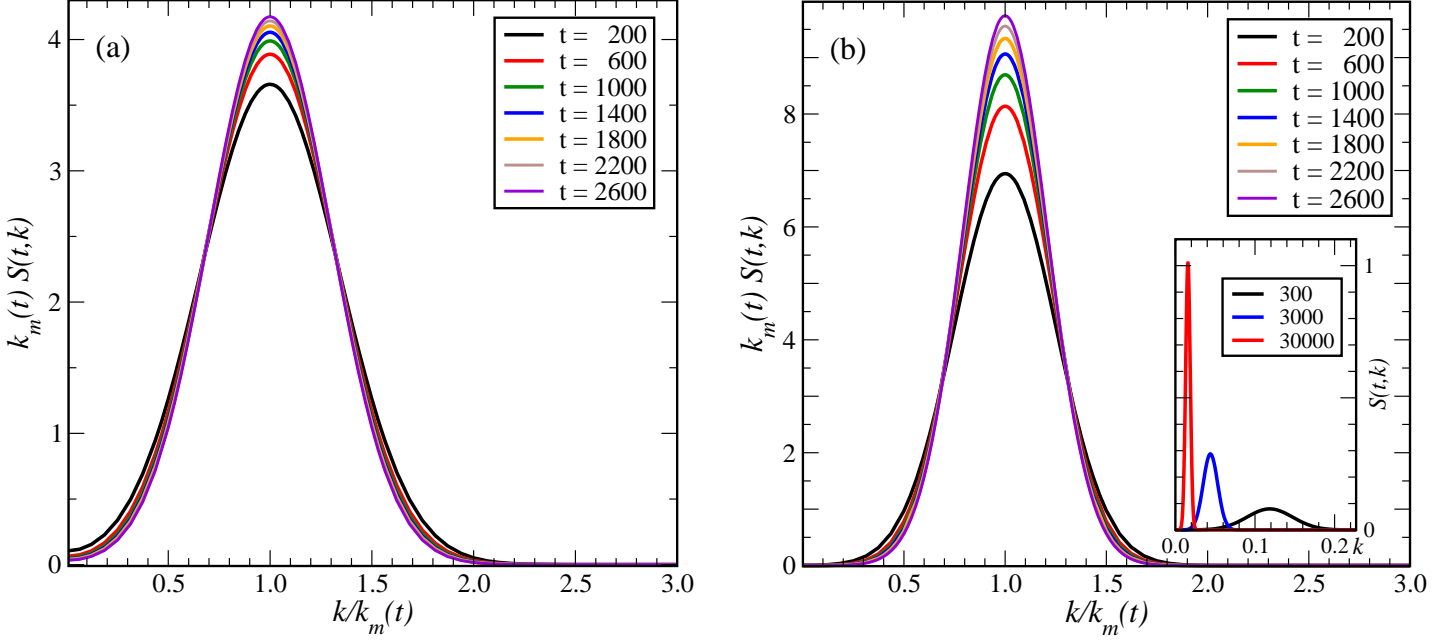


Figure 2: Scaled structure factor $S(t, k)$, normalised to $S(1, 0) = 1$, for (a) the slope-slope correlations in the second model and (b) the height-height correlations in the third model, for several times t and at temperature $T = 0$. In the inset in (b) also shows the unscaled structure factor (arbitrary units), for several times t .

In particular, this gives the equal-time correlator

$$\begin{aligned}
 C_n(t) &:= C_n(t, t) = e^{-4\nu t} I_n \left(4\nu t \sqrt{1 + \left(\frac{Z(t)}{2\nu t} \right)^2} \right) \cos \left(n \arctan \frac{Z(t)}{2\nu t} \right) \\
 &\stackrel{t \rightarrow \infty}{\simeq} C_0(t, t) \exp \left(- \left(\frac{n}{L_1(t)} \right)^2 \right) \cos \left(\frac{n}{L_2(t)} \right)
 \end{aligned} \tag{4.11}$$

with the equal-time autocorrelator $C_0(t) := C_0(t, t)$ and the two distinct length scales

$$L_1(t) := \sqrt{8\nu t} \quad , \quad L_2(t) := \sqrt{\frac{4\nu}{\kappa_1} \frac{t}{\ln(\kappa_2 t) F(t)}} \tag{4.12}$$

where $F(t)$ is defined in appendix B and gives double-logarithmic corrections to scaling for the third model. The presence of two logarithmically different length scales indicates a breaking of dynamical scaling. This becomes even more explicit when considering the structure factor

$$\begin{aligned}
 S(t, k) &= \frac{1}{\sqrt{2\pi}} \int_{\mathbb{R}} dn e^{-ikn} C_n(t) \\
 &= \frac{C_0(t) L_1(t)}{\sqrt{2}} \exp \left(- \frac{1}{4} \frac{L_1^2(t)}{L_2^2(t)} \right) \exp \left(- \frac{L_1^2(t)}{4} k^2 \right) \cosh \left(\frac{L_1(t)}{L_2(t)} \frac{L_1(t) k}{2} \right) \\
 &\simeq \frac{C_0(t) L_1(t)}{\sqrt{2} (\kappa_2 t)^{\kappa_1/2}} e^{-(L_1(t) k/2)^2} \cosh \left(\frac{L_1(t)}{L_2(t)} \frac{L_1(t) k}{2} \right) \begin{cases} 1 & ; \text{second model} \\ \frac{3e^{1/2}}{2} \ln \kappa_2 t & ; \text{third model} \end{cases}
 \end{aligned} \tag{4.13}$$

where the last logarithmic factor comes from the auxiliary function $F(t)$. Working out the long-time behaviour of the two lengths, we find, for the second and third model, respectively

$$S^{(II)}(t, k) = S^{(0)} e^{-2\nu t k^2} \cosh \left(\sqrt{4\nu t \ln 8\pi\nu t} k \right) \quad (4.14a)$$

$$S^{(III)}(t, k) = S^{(0)} e^{-2\nu t k^2} \left(\frac{\ln^{3/2} \kappa_2 t}{t} \right) \cosh \left(k \sqrt{4\nu t \left(3 \ln \kappa_2 t - 2 \ln(\ln \kappa_2 t) - \left(1 + 2 \ln \frac{3}{2} \right) \right)} \right) \quad (4.14b)$$

with known constants $S^{(0)}$ and κ_2 was defined above.

The explicit expressions (4.14) permit a clear understanding of the distinct length scales involved. Since for both models, the structure factor contains two factors with different k -dependence, one expects a peak at some time-dependent *lieu* $k_m(t)$. Figure 2 shows that this indeed the case, notably in the inset of figure 2b, which illustrates how for increasing times the peak becomes sharper and is progressively shifted towards $k \rightarrow 0$. Eq. (4.13) implies that $k_m(t) \simeq L_2^{-1}(t) \sim \left(\frac{\ln t}{t} \right)^{1/2}$. If one attempts to scale the structure factors with respect to $L_2(t)$, as is done in figure 2ab, one might believe at first sight that a scaling behaviour would result (at least for the second model). However, the presence of the diffusive length $L_1(t) \sim t^{1/2}$, it is impossible to achieve a collapse and dynamical scaling does *not* hold for *all* wave numbers $k \geq 0$.¹¹ This kind of behaviour is completely analogous to the one of phase-separation in the $T = 0$ kinetic spherical model with a conserved order-parameter (model B dynamics) [14, 5]. These two length scales also describe the time-space correlator: while L_2 is seen in the spatial modulation, the scale L_1 describes the overall spatial decay.

The scaling of the autocorrelator introduces at least one more scale $L_{\text{corr}}(t) \sim (t / \ln^\vartheta t)^{1/2}$, with $\vartheta \geq \frac{1}{2}$. Several distinct regimes must be distinguished, as we shall see in section 5.

4.3 Zero-temperature response

From (3.27,3.28), we have for large times the factorisation into the autoresponse

$$R(t, s) = e^{-2\nu(t-s)} I_0 \left(2\nu(t-s) \sqrt{1 + \left(\frac{Z(t) - Z(s)}{2\nu(t-s)} \right)^2} \right) \quad (4.15)$$

and the time-space response

$$\begin{aligned} R_n(t, s) &= e^{-2\nu(t-s)} I_n \left(2\nu(t-s) \sqrt{1 + \left(\frac{Z(t) - Z(s)}{2\nu(t-s)} \right)^2} \right) \cos \left(n \arctan \frac{Z(t) - Z(s)}{2\nu(t-s)} \right) \\ &\simeq R(t, s) \exp \left[-\frac{1}{2} \left(\frac{n}{\sqrt{2\nu(t-s)}} \right)^2 \right] \end{aligned} \quad (4.16)$$

¹¹In the third model, scaling is further broken by an additional logarithmic factor.

The scaling is obtained as follows and corresponds to (4.8).¹² We have for the time difference

$$\tau = t - s = \frac{s}{\ln(\kappa_2 s)} W((y-1) \ln^{1-\vartheta}(\kappa_2 s)) \quad (4.17)$$

where $\vartheta > 1$, in terms of Lambert's W function. This gives $\tau \sim (y-1)s \ln^{-\vartheta}(\kappa_2 s)$ for large times. The autoresponse (3.27) takes the scaling form

$$R(t, s) = (4\pi\nu s)^{-1/2} \ln^{\vartheta/2}(\kappa_2 s) (y-1)^{-1/2} \quad (4.18)$$

which is so close to the one found in systems undergoing simple ageing (as the first Arcetri model, see appendix A), up to a logarithmic prefactor, that we read off the exponents $a = -\frac{1}{2}$ and $\lambda_R/z = \frac{1}{2}$, see table 1. There is no correspondence in the autoresponse to the scaling (4.6) of the autocorrelator.

We also observe that the response $\mathcal{R}_n(t, s)$ defined in (3.29) has the same factorisation into the autoresponse $\mathcal{R}(t, s)$ and a spatial part as in (3.28). The autoresponse is readily found and reads, in the scaling limit with $\vartheta > 1$

$$\mathcal{R}(t, s) = (8\pi^{1/2}\nu s)^{-1} \ln^{(1+\vartheta)/2}(\kappa_2 s) (y-1)^{-1/2} \quad (4.19)$$

and we read off $a_{\mathcal{R}} = 0$ and $\lambda_{\mathcal{R}} = 1$.

In the time-space responses, we merely find a single further length scale $L_{\text{diff}}(t) \sim t^{1/2}$, which describes the overall decay, but no spatial modulation of the response.

5 Discussion and perspectives

Triggered by an analogy with the spherical model of a ferromagnet [7], we have used the Burgers and Kardar-Parisi-Zhang equations to define two new models, which we have called the *second Arcetri model* and the *third Arcetri model*, see sections 2.2 and 2.3. Because of the natural initial conditions (2.6) and (2.11), respectively, the second model is interpreted as a lattice gas model, whereas the third model appears to describe a growing interface. We have found exactly, at vanishing ‘temperature’ $T = 0$, the exact two-time correlators and responses. Unexpectedly, the scaling behaviour of these turned out not to be given by simple ageing, but rather by a subtle modification of this, described by *logarithmic sub-ageing* and characterised by the presence of several logarithmically distinct time-dependent length scales.

As we shall see now, this is a very fortunate circumstance, since the separation of several length scales, which coalesce for simple ageing, allows for a much more clear understanding how the ageing process takes place. Figure 3 summarises this as a kinetic phase diagram.

Equations in physics should be read as instructions how to carry out experiments. In the case of ageing, the central equation describes the scaling of the difference between *observation time* t and *waiting time* s :

$$\tau = t - s = \frac{s}{\ln^{\vartheta} s} f(s, y) \stackrel{s \rightarrow \infty}{\simeq} \frac{s}{\ln^{\vartheta} s} (y-1) \quad (5.1)$$

¹²The only difference between the second and third model is a logarithmic modification of the scaling variable, as explained in appendix C, and which disappears asymptotically for times $t, s \gg 1$.

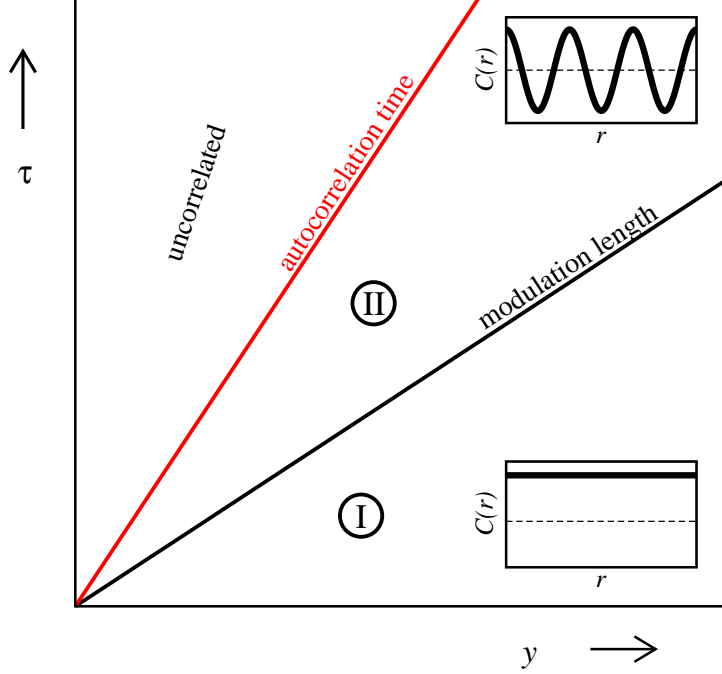


Figure 3: Schematic kinetic phase diagram of the second and third Arcetri models at temperature $T = 0$. The regions of distinct scaling behaviour for time differences $\tau = t - s = \tau(s, y)$ are indicated. The spatial behaviour of the single-time correlator is shown in the insets for the phases I and II.

in terms of a certain function $f = f(s, y)$ which we have determined explicitly, for the second and third Arcetri models, in section 4. In combination with the scaling form of the autocorrelator $C = C(t, s)$ or the autoresponse $R = R(t, s)$, the meaning of eq. (5.1) is:

“For a large waiting time s , and a fixed scaling variable $y > 1$, compute the observation-time scale $t = s + \tau(s, y)$ in order to observe the corresponding scaling behaviour of the observable in question.”.

For systems with logarithmic sub-ageing, as it is realised in the second and third Arcetri models at $T = 0$, this leads to the following insights:

1. Phase I is characterised by an exponent $\vartheta > 1$ in (5.1).¹³ Both correlators and responses scale, and the asymptotic forms of the scaling variables are compatible. The scaling functions are given by eqs. (4.9) and (4.18), respectively and the corresponding exponents are listed in tables 1 and 2. These relatively small time differences also imply a corresponding length scale $L_{\text{corr}}(t) \sim \sqrt{t/\ln^\vartheta t}$. On these time and space scales, the autocorrelation is perfect and the system is spatially homogeneous. The most rapid events occur in the slow decay of the response to an external, localised perturbation.
2. The end of phase I is seen when one goes to larger scales by choosing $\vartheta = 1$. At this length scale, which seen from phase I would correspond to a $y \rightarrow \infty$ limit, the responses have decayed. The new feature is the onset of spatial modulation of the spatial correlators

¹³The precise scaling prescriptions are given by (4.8, 4.17), see also figure 4.

(4.11), which occurs at the scale $L_{\max} \sim \sqrt{t/\ln t}$, and signalled by a strong peak in the structure function at wave number k_{\max} , see figure 3. Since the scale $L_{\text{diff}}(t) \gg L_{\max}(t)$, these modulations occur with constant amplitude. And because the scaling form (4.8) of the autocorrelator still holds, autocorrelations do not dissipate away.

3. Phase II is characterised by the intermediate range $\frac{1}{2} < \vartheta < 1$, between the onset of spatial modulations and a new scaling form of the autocorrelator, which in this scaling limit is still perfect. In contrast to phase I, the responses have at this time-scale decayed away and do not scale anymore.
4. The end of phase II is seen at large length scales $L_{\text{corr}}(t)$ which correspond to $\vartheta = \frac{1}{2}$. At these scales, the system consists of many small spatial units, each of them still fully ordered. Now the autocorrelator decays according to the scaling form (4.6), but since still $L_{\text{diff}} \gg L_{\text{corr}}(t)$, each spatial unit remains fully ordered. Responses to external perturbations are vanishingly small on these scales.
5. On scales so large that they correspond to $0 < \vartheta < \frac{1}{2}$, there is no more scaling form and temporal correlations are lost. The eventual decay of the amplitude of spatial correlations at distances corresponding to $\vartheta = 0$ has no effect on a system which at these scales is already disordered.

A completely analogous behaviour can be found in the kinetic spherical model with a conserved order parameter (model B dynamics) at temperature $T = 0$, which describes spinodal decomposition, in $d > 2$ dimensions. It has a dynamical exponent $z = 4$, hence is distinct from the Arcetri models. However, the breaking of scale-invariance of the equal-time spin-spin correlator, through two logarithmically distinct length scales, is analogous to (4.11) [14]. Furthermore, the scaling of the magnetic autocorrelator $C(t, s)$ and of the magnetic autoresponse $R(t, s)$ [9] is completely analogous to the Arcetri models. The scaling variable is, again, defined by $\tau = t - s = (y - 1)s \ln^{-\vartheta} s$. If $\vartheta > 1$, for s sufficiently large, we find the autocorrelator $C(t, s) = 1$ and the autoresponse $R(t, s) \sim s^{-(d+2)/4} \left(\ln^{\vartheta(d+2)/4} s \right) (y - 1)^{-(d+2)/4}$. If $\frac{1}{2} < \vartheta < 1$, one still has $C(t, s) \sim \exp \left(-\frac{d}{64}(y - 1)^2 \ln^{1-2\vartheta} s \right) \xrightarrow{s \rightarrow \infty} 1$ and the autoresponse does not scale. Finally, for $\vartheta = \frac{1}{2}$, one has $C(t, s) \sim \exp \left(-\frac{d}{64}(y - 1)^2 \right)$ [9].¹⁴ See also table 2.

Logarithmic sub-ageing might also occur in the ageing of glassy materials. It is common to fit experimental data on relaxation phenomena in glasses through sub-ageing, with a sub-ageing exponent $\mu \lesssim 1$, see [72, 79] and refs. therein, which in practise may become very difficult to distinguish from a logarithmic subageing [9].

¹⁴The presence of two logarithmically different length scales is called *multiscaling* [14]. In $O(n)$ -symmetric magnets with a conserved order-parameter, quenched to temperature $T = 0$, multiscaling only occurs exactly in the spherical limit $n = \infty$ but does not arise for n finite [5, 6, 59]. It appears plausible that a similar effect may also arise for the second and third Arcetri models at $T = 0$, in view of the conservation law (2.8). Multiscaling has been argued to be present in systems such as diffusion-limited aggregation (DLA) [15], but apparently no consensus has been reached on whether multiscaling in DLA is genuine [61] or rather an effective finite-size effect [71, 60].

A slightly different situation arises in the *quantum* dynamics of the quantum spherical model, where the associated Lindblad equation preserves the canonical commutator relations, which might be viewed as an (infinite) set of prescribed conservation laws. Then, at $T = 0$ and for quantum quenches deep into the two-phase coexistence region, a simple scaling behaviour without logarithmic corrections is found for $d = 2$ dimensions, but multiscaling arises for $d \neq 2$ [80].

Our discussion has been restricted to the special case $T = 0$. The solution of the spherical constraint for $T > 0$ is left as an open problem. Since the conservation laws (2.8) of the second model are maintained for $T \neq 0$, one might anticipate that a sufficiently small change in T should not lead to a drastic modification of the qualitative behaviour of the second model. In the third model, however, for any $T > 0$ the conservation laws (2.8) are broken and in consequence, the behaviour of the model should change notably. Another question left open is the extension to any dimension d .

Appendix A. The first Arcetri model revisited

We recall and extend the so-called ‘first’ Arcetri model, as originally introduced in [39], in order to clarify the possible interpretations, either as a model of interface growth or else of interacting particles. For brevity of notation, we restrict to $d = 1$ dimensions.

A model of growing interfaces is naturally described in terms of the height $h_n(t)$ at the site n of a periodic chain with N sites. The defining equation of motion of the *first Arcetri model for the heights* (ARCTRI 1H) is, along with the spherical constraint on the slopes

$$\partial_t h_n(t) = \nu (h_{n+1}(t) + h_{n-1}(t) - 2h_n(t)) + \mathfrak{z}(t)h_n(t) + \eta_n(t) \quad (\text{A.1})$$

$$\frac{1}{4} \sum_{n=0}^{N-1} \langle\langle (h_{n+1}(t) - h_{n-1}(t))^2 \rangle\rangle = N \quad (\text{A.2})$$

Herein, to each lattice site n a centred gaussian random variable $\eta_n(t)$ is attached, with variance $\langle\eta_n(t)\eta_m(t')\rangle = 2\nu T\delta(t-t')\delta_{n,m}$. The Lagrange multiplier $\mathfrak{z}(t)$ is determined from the ‘spherical constraint’ (A.2) and ν and T are constants. A natural initial condition stipulates an initial gaussian distribution, with spatially translation-invariant moments

$$\langle\langle h_n(0) \rangle\rangle = H_0, \quad \langle\langle h_n(0)h_m(0) \rangle\rangle - \langle\langle h_n(0) \rangle\rangle \langle\langle h_m(0) \rangle\rangle = H_1 \delta_{n,m} \quad (\text{A.3})$$

This describes an initially flat interface of uncorrelated heights and of initial mean height H_0 .

If one re-writes the equation of motion (A.1) in terms of the slopes $u_n(t) := \frac{1}{2}(h_{n+1}(t) - h_{n-1}(t))$, one has

$$\partial_t u_n(t) = \nu (u_{n+1}(t) + u_{n-1}(t) - 2u_n(t)) + \mathfrak{z}(t)u_n(t) + \frac{1}{2}(\eta_{n+1}(t) - \eta_{n-1}(t)) \quad (\text{A.4})$$

$$\sum_{n=0}^{N-1} \langle\langle u_n(t)^2 \rangle\rangle = N \quad (\text{A.5})$$

which together with the initial conditions (A.3), with $H_0 = 0$, was the only model studied in [39]. The formal continuum limit of (A.4) is given by (1.4). The *first Arcetri model for the particles* (or slopes) (ARCTRI 1U) has the defining equation of motion (A.4), the spherical constraint (A.5) and an initial gaussian distribution, with the moments

$$\langle\langle u_n(0) \rangle\rangle = 0, \quad \langle\langle u_n(0)u_m(0) \rangle\rangle = U_1 \delta_{n,m} \quad (\text{A.6})$$

This initial condition with zero average slope corresponds to a system of initially uncorrelated particles with average mean density $\varrho = \frac{1}{2}$.

The solution of the equations of motion is standard, see [39]. Let $g(t) := \exp\left(-2 \int_0^t d\tau \mathfrak{z}(\tau)\right)$, and define as well

$$\begin{aligned} f(t) &:= \frac{1}{2\pi} \int_{-\pi}^{\pi} dp \sin^2 p e^{-4\nu(1-\cos p)t} = \frac{e^{-4\nu t} I_1(4\nu t)}{4\nu t} \\ F(t) &:= \frac{1}{2\pi} \int_{-\pi}^{\pi} dp e^{-4\nu(1-\cos p)t} = e^{-4\nu t} I_0(4\nu t) \end{aligned} \quad (\text{A.7})$$

where the I_n are modified Bessel functions [1]. For $d \geq 1$ dimensions, these functions become [39]

$$f(t) = d \frac{e^{-4\nu t} I_1(4\nu t)}{4\nu t} \left(e^{-4\nu t} I_0(4\nu t) \right)^{d-1}, \quad F(t) = \left(e^{-4\nu t} I_0(4\nu t) \right)^d \quad (\text{A.8})$$

The spherical constraints (A.2,A.5) reduce to the Volterra integral equations

$$\begin{cases} g(t) = H_1 f(t) + 2\nu T \int_0^t d\tau g(\tau) f(t-\tau) & ; \text{ for ARCETRI 1H} \\ g(t) = U_1 F(t) + 2\nu T \int_0^t d\tau g(\tau) f(t-\tau) & ; \text{ for ARCETRI 1U} \end{cases} \quad (\text{A.9})$$

which gives immediately for the Laplace transformation $\bar{g}(p) = \int_0^\infty dt e^{-pt} g(t)$

$$\bar{g}(p) = \begin{cases} H_1 \bar{f}(p) / [1 - 2\nu T \bar{f}(p)] & ; \text{ for ARCETRI 1H} \\ U_1 \bar{F}(p) / [1 - 2\nu T \bar{f}(p)] & ; \text{ for ARCETRI 1U} \end{cases} \quad (\text{A.10})$$

such that the small- p behaviour of $\bar{g}(p)$ is related by a Tauberian theorem to the long-time asymptotics of $g(t)$ for $t \rightarrow \infty$ [25]. This gives two distinct physical situations:

(a) If an interpretation in terms of interface growth is sought, one may consider the ARCETRI 1H model, characterised by initially uncorrelated height variables according to (A.3). Then the time-dependent height is

$$\langle\langle h_n(t) \rangle\rangle = H_0 g(t)^{-1/2} \quad (\text{A.11})$$

This average is indeed non-vanishing, since the equation of motion (A.1) is not invariant under the transformation $h_n(t) \mapsto h_n(t) + \alpha$. The two-time autocorrelator is given by

$$\begin{aligned} C(t, s) &:= \langle\langle (h_n(t) - \langle\langle h_n(t) \rangle\rangle) (h_n(s) - \langle\langle h_n(s) \rangle\rangle) \rangle\rangle \\ &= \frac{H_1 F((t+s)/2)}{\sqrt{g(t)g(s)}} + 2\nu T \int_0^{\min(t,s)} d\tau \frac{g(\tau)}{\sqrt{g(t)g(s)}} F\left(\frac{t+s}{2} - \tau\right) \end{aligned} \quad (\text{A.12})$$

such that the interface width becomes

$$w^2(t) = C(t, t) = \frac{H_1 F(t)}{g(t)} + 2\nu T \int_0^t d\tau \frac{g(\tau)}{g(t)} F(t - \tau) \quad (\text{A.13})$$

Finally, the linear autoresponse of the height $h_n(t)$ with respect to a change $h_n(s) \mapsto h_n(s) + j_n(s)$ in the height is independent of the initial distribution and reads

$$R(t, s) := \left. \frac{\delta \langle h_n(t) \rangle}{\delta j_n(s)} \right|_{j=0} = \Theta(t-s) \sqrt{\frac{g(s)}{g(t)}} F\left(\frac{t-s}{2}\right) \quad (\text{A.14})$$

where the Heaviside function $\Theta(t)$ expresses causality. Eqs. (A.12,A.14) are the analogues of (3.34,3.35) in the third model, for $n = 0$.¹⁵

(b) If a comparison with the 1D TASEP is sought, one may consider the ARCETRI 1U model, characterised by initially uncorrelated slopes and described by (A.6). The slope-slope autocorrelator $C(t, s)$, related to the connected density-density correlator via (1.13), the linear

¹⁵In the KPZ universality class, the KPZ *ansatz* stipulates that $\langle\langle h_n(t) \rangle\rangle - v_\infty t \sim t^\beta$ and $w(t) \sim t^\beta$ scale both with the same exponent β [66], and where v_∞ is the mean velocity of particle deposition (one may achieve $v_\infty = 0$ by the choice of a co-moving frame of reference, implicit in (1.1)). The KPZ ansatz is satisfied by the Arcetri 1H model at $T = T_c$, but does not hold for $T < T_c$. In the third Arcetri model at $T = 0$, the KPZ ansatz is broken through logarithmic sub-scaling exponents, see section 4.

auto-response $R(t, s)$ of the slope $u_n(t)$ with respect to a change $u_n(s) \mapsto u_n(s) + k_n(s)$ in the slope, and the linear auto-response $\mathcal{R}(t, s)$ of the slope $u_n(t)$ with respect to a change $j_n(s)$ in the height, respectively, are given by

$$\begin{aligned}
C(t, s) &:= \langle\langle u_n(t)u_n(s) \rangle\rangle = \frac{U_1 F((t+s)/2)}{\sqrt{g(t)g(s)}} + 2\nu T \int_0^{\min(t,s)} d\tau \frac{g(\tau)}{\sqrt{g(t)g(s)}} f\left(\frac{t+s}{2} - \tau\right) \\
R(t, s) &:= \left. \frac{\delta \langle u_n(t) \rangle}{\delta k_n(s)} \right|_{k=0} = \Theta(t-s) \sqrt{\frac{g(s)}{g(t)}} F\left(\frac{t-s}{2}\right) \\
\mathcal{R}(t, s) &:= \left. \frac{\delta \langle u_n(t) \rangle}{\delta j_n(s)} \right|_{j=0} = \Theta(t-s) \sqrt{\frac{g(s)}{g(t)}} f\left(\frac{t-s}{2}\right)
\end{aligned} \tag{A.15}$$

Eq. (A.15) gives the analogues of (3.21,3.27,3.29) in the second model.

Following the analysis in [39], the critical exponents are readily found and are listed in tables 1 and 2.

Appendix B. Long-time correlator

We derive the long-time behaviour of the correlations in the second and third model, at $T = 0$.

In what follows, we shall often need the following asymptotic formula [1, 70]

$$I_n(x) \simeq \frac{1}{\sqrt{2\pi x}} \exp\left(x - \frac{4n^2 - 1}{8x}\right) (1 + O(x^{-2})) \tag{B.1}$$

First, we must find $Z(t)$ for large times from the constraint (3.15) or (3.33), respectively. We now prove eq. (4.3) in the main text.

For the second model, (3.15) becomes (4.1). Since the Bessel function $I_0(x)$ is monotonically increasing with $x > 0$, this implies that $Z(t)$ increases with $t > 0$. Then, one can apply (B.1) and one has

$$\begin{aligned}
e^{4\nu t} &= I_0\left(4\nu t \sqrt{1 + \frac{Z^2(t)}{4\nu^2 t^2}}\right) \simeq \frac{\exp 4\nu t \sqrt{1 + \frac{Z^2(t)}{4\nu^2 t^2}}}{\left[8\pi\nu t \sqrt{1 + \frac{Z^2(t)}{4\nu^2 t^2}}\right]^{1/2}} \\
&\simeq \exp\left[4\nu t \left(1 + \frac{Z^2(t)}{8\nu^2 t^2}\right) - \frac{1}{2} \ln(8\pi\nu t) - \frac{1}{2} \ln\left(1 + \frac{Z^2(t)}{8\nu^2 t^2}\right)\right]
\end{aligned}$$

Keeping the terms of leading non-vanishing order, gives a linear equation for $Z^2(t)$

$$\frac{Z^2(t)}{2\nu t} - \frac{1}{2} \ln(8\pi\nu t) = 0$$

equivalent to the first eq. (4.3) in the main text. One might obtain this result as well from the integral representation of \mathcal{J}_0 , by the saddle-point method.

For the third model, the constraint (3.33) takes the form, using appendix D and standard formulæ for the modified Bessel function [1]

$$\begin{aligned} & \left[I_1 \left(\sqrt{(4\nu t)^2 + (2Z(t))^2} \right) (4\nu t)^2 \right. \\ & \left. + 2Z(t)^2 \sqrt{(4\nu t)^2 + (2Z(t))^2} \left(I_0 \left(\sqrt{(4\nu t)^2 + (2Z(t))^2} \right) + I_2 \left(\sqrt{(4\nu t)^2 + (2Z(t))^2} \right) \right) \right] \\ & = e^{4\nu t} [(4\nu t)^2 + (2Z(t))^2]^{-3/2} \end{aligned} \quad (\text{B.2})$$

As before, we use (B.1) and expand to the lowest required order. We then find

$$e^{4\nu t} [(4\nu t)^2 + (2Z(t))^2]^{-3/2} = \frac{\exp 4\nu t \sqrt{1 + \frac{Z^2(t)}{4\nu^2 t^2}}}{\left[8\pi\nu t \sqrt{1 + \frac{Z^2(t)}{4\nu^2 t^2}} \right]^{1/2}} [(4\nu t)^2 + (2Z(t))^2 4\nu t]$$

which can be further simplified into

$$\frac{Z(t)^2}{2\nu t} - \frac{1}{2} \ln(2\pi) - \frac{7}{2} \ln(4\nu t) + \ln \left((4\nu t)^2 \left(1 + \frac{(2Z(t))^2}{4\nu t} \right) \right) = 0$$

The single positive solution of this equation is

$$Z(t) = \sqrt{2tW \left((32\pi e)^{1/2} t^{3/2} \right) - t} \quad (\text{B.3})$$

where $W(x)$ denotes Lambert's W -function, defined as the solution of $We^W = x$ [55, 16]. Throughout, we shall require the following two expansions of Lambert's function

$$W(x) \simeq \begin{cases} x - x^2 + O(x^3) & ; \text{ for } x \rightarrow 0 \\ \ln x - \ln(\ln x) + O(\ln(\ln x)/\ln(x)) & ; \text{ for } x \rightarrow \infty \end{cases} \quad (\text{B.4})$$

Inserting into (B.3), we finally have the leading asymptotics for $Z(t)$, including the dominant logarithmic corrections

$$Z(t) \simeq \sqrt{3t \ln(\kappa_2 t) \left[1 - \frac{2 \ln(\frac{3}{2} \ln \kappa_2 t)}{\ln \kappa_2 t} - \frac{1}{3 \ln \kappa_2 t} \right]} =: \sqrt{3t \ln(\kappa_2 t) F(t)} \quad (\text{B.5})$$

and we have derived eqs. (4.3,4.4) in the main text, and especially the values of κ_1 and κ_2 quoted therein. For later use, below and in appendix C, we also defined the function $F(t)$. This function describes additional modifications of the scaling behaviour of the third model with respect to the second model, where from the constraint (4.1) we had seen that $F(t) = 1$.

Since the abstract expression (3.21) holds true for both the slope correlator in the second model and the height correlator in the third model, respectively, both can be analysed together. We begin with an analysis of the scaling behaviour of the autocorrelator, which reads

$$C(t, s) = e^{-2\nu(t+s)} I_0 \left(2\nu(t+s) \sqrt{1 + \left(\frac{Z(t) + Z(s)}{2\nu(t+s)} \right)^2} \right) \quad (\text{B.6})$$

In what follows, we shall use the logarithmic subageing scaling variable

$$\tau = t - s = \frac{s}{\ln^\vartheta \kappa_2 s} (y - 1) g(s) \quad (\text{B.7})$$

which is to be considered in the double limit $t, s \rightarrow \infty$ such that $y > 1$ is being kept fixed, and a positive constant $\vartheta > 0$, in analogy with, but generalising [9]. In certain cases, as we shall see especially in appendix C when analysing the autoresponse function, the function $g(s)$ has to be conveniently chosen. For what follows, an important simplification is obtained for the auxiliary function $F(t)$. Inserting the scaling ansatz and expanding, we find

$$F(t) \simeq 1 - \frac{2 \ln \frac{3}{2} - 1}{6 \ln \kappa_2 s} - \frac{1}{3} \frac{\ln \ln \kappa_2 s}{\ln \kappa_2 s} + \text{O}(\ln^{-2} \kappa_2 s) \simeq F(s) \quad (\text{B.8})$$

to this order.

Our first scaling analysis uses again (B.1), and (4.3). We find by expansion, up to the first non-vanishing order, and using (B.8)

$$\begin{aligned} \ln C(t, s) &\simeq \frac{(Z(t) + Z(s))^2}{4\nu(t+s)} - \frac{1}{2} \ln(4\pi\nu(t+s)) + \text{O}(s^{-1}, t^{-1}) \\ &\simeq F(s) \frac{(\sqrt{\kappa_1 \nu t \ln \kappa_2 t} + \sqrt{\kappa_1 \nu s \ln \kappa_2 s})^2}{4\nu(t+s)} - \frac{1}{2} \ln(4\pi\nu(t+s)) \end{aligned} \quad (\text{B.9})$$

We use the scaling ansatz (B.7). Inserting into the above, and expanding, we obtain

$$\begin{aligned} \ln C(t, s) &\simeq -\frac{1}{2} \ln(8\pi\nu) + \frac{\kappa_1}{2} \ln \kappa_2 + \frac{1}{2} (\kappa_1 - 1) \ln s - \frac{\kappa_1}{32} (y - 1)^2 \ln^{1-2\vartheta}(\kappa_2 s) \\ &\quad - \delta_{\kappa_1,3} \left(\frac{1}{2} \ln \ln \kappa_2 s + \frac{1}{4} \left(2 \ln \frac{3}{2} - 1 \right) \right) + \text{o}(1) \end{aligned}$$

where the contributions in the second line only arise for the third model. Multiscaling can only be avoided by choosing $\vartheta = \frac{1}{2}$ [9]. This gives (4.6,4.7) in the main text and is the first type of scaling behaviour of $C(t, s)$ to be considered.

However, different ways to obtain a scaling behaviour exist. These are found by considering the difference $\tau = t - s$ between the two times and by making the change of variables

$$\tau = t - s = \frac{s}{\ln^\vartheta(\kappa_2 s)} f(s, y) \quad (\text{B.10})$$

where the unknown function $f = f(s, y)$ is assumed to be small compared to $\ln^\vartheta s$. The function $f = f(s, y)$ must be found such that $\tau = \tau(y)$ is monotonically increasing with y and the autocorrelator $C = C(y)$ is monotonically decreasing. Of course, the relation (B.10) is to be understood in the scaling limit $t, s \rightarrow \infty$ with y being kept fixed. Using again (B.9) and expanding as before, we have

$$\ln C(t, s) \simeq \frac{\kappa_1 - 1 - \delta_{\kappa_1,3}}{2} \ln(\ln \kappa_2 s) - \frac{\kappa_1}{32} \ln^{1-2\vartheta}(\kappa_2 s) f^2(s, y) - \frac{\delta_{\kappa_1,3}}{4} \left(2 \ln \frac{3}{2} - 1 \right) \quad (\text{B.11})$$

In order to obtain a scaling behaviour, we make the following ansatz

$$\ln C(t, s) \stackrel{!}{=} A' \ln(\ln \kappa_2 s) - \ln(y - 1) + \frac{1}{2} \ln f^2(s, y) - \frac{B'}{32} \ln^{1-2\vartheta}(\kappa_2 s) f(s, y) - \frac{\delta_{\kappa_1,3}}{4} \left(2 \ln \frac{3}{2} - 1 \right) \quad (\text{B.12})$$

where the constants A', B' are to be determined. Consistency between (B.11) and (B.12) gives the condition

$$f^2 \exp \left[\frac{\kappa_1 - B'}{16} \ln^{1-2\vartheta}(\kappa_2 s) f^2 \right] = (y-1)^2 \ln^{\kappa_1 - 2A' - 1 - \delta_{\kappa_1,3}}(\kappa_2 s) \quad (\text{B.13})$$

which has the unique solution

$$f^2 = \frac{16}{\kappa_1 - B'} \ln^{1-2\vartheta}(\kappa_2 s) W \left(\frac{\kappa_1 - B'}{16} (y-1)^2 \ln^{\kappa_1 - 2A' - 2\vartheta - \delta_{\kappa_1,3}}(\kappa_2 s) \right) \quad (\text{B.14})$$

using again the Lambert- W function. Herein, self-consistency requires that $\kappa_1 - B' > 0$ and $\kappa_1 - 2A' - 2\vartheta - \delta_{\kappa_1,3} < 0$. Then, we find the following asymptotic form, for $s \rightarrow \infty$

$$\tau = t - s = \frac{s}{\ln^{(1+\delta_{\kappa_1,3}-\kappa_1)/2+A'+\vartheta}}(\kappa_2 s)} (y-1) \quad (\text{B.15})$$

and we see that at least for the autocorrelator, we can simply set $g(s) = 1$. This explains the chosen ansatz: we have chosen variables such that in the special case where $(1 + \delta_{\kappa_1,3} - \kappa_1)/2 + A' + \vartheta = 0$, we recover the scaling form $\tau = t - s = s(y-1)$ of simple ageing. This discussion will be completed by a comparison with the corresponding results from the autoresponse $R(t, s)$, see appendix C.

In order to derive (3.22), we reuse eq. (B.1) in (3.21) and also recall that for large times, $Z(t) \sim t^{1/2}$, up to logarithmic factors. All factors which do not contain n will be absorbed into the autocorrelator $C(t, s)$. Therefore, the leading n -dependent term coming from the Bessel function I_n in (3.21) is simply $\exp[-n^2/(4\nu(t+s))]$, whereas those terms which contain $Z(t)$ or $Z(s)$ will give rise to finite-time corrections to the leading scaling contribution. Hence (3.22) describes the leading scaling behaviour of the time-space correlator $C_n(t, s)$.

In order to derive the spatial modulation of the time-space correlator (4.10), we start from (3.22). For large times $t, s \rightarrow \infty$, the modulating factor can be rewritten as follows

$$\cos \left(n \frac{Z(t) + Z(s)}{2\nu(t+s)} \right) = \cos \left(\frac{n}{\sqrt{2\nu(t+s)}} \sqrt{\frac{(Z(t) + Z(s))^2}{2\nu(t+s)}} \right)$$

Herein, since $Z(t) \sim t^{1/2}$, we used that the argument of the arctan is small so that it is enough to keep the lowest order. Now, straightforward expansion of the square root produces the stated form (which is symmetric in t and s) and which can be done, up to finite-time corrections.

Finally, the single-time correlator $C_n(t, t) = \lim_{s \rightarrow t} C_n(t, s)$ is read off immediately from (4.10) to produce (4.11).

Appendix C. Long-time response

The analysis of the autoresponse starts from

$$R(t, s) = e^{-2\nu(t-s)} I_0 \left(2\nu(t-s) \sqrt{1 + \left(\frac{Z(t) - Z(s)}{2\nu(t-s)} \right)^2} \right) \quad (\text{C.1})$$

Expanding the Bessel function via (B.1) and using (4.3,4.4,B.7), we obtain

$$\begin{aligned}\ln R(t, s) &\simeq \frac{(Z(t) - Z(s))^2}{4\nu(t-s)} - \frac{1}{2} \ln(4\pi\nu(t-s)) + O(s^{-1}, t^{-1}) \\ &\simeq F(s) \frac{(\sqrt{\kappa_1 \nu t \ln \kappa_2 t} - \sqrt{\kappa_1 \nu s \ln \kappa_2 s})^2}{4(t-s)} - \frac{1}{2} \ln(4\pi\nu(t-s))\end{aligned}\quad (\text{C.2})$$

In analogy with our analysis for the autocorrelator in appendix B, we try to find a scaling variable y such that the time difference $\tau = \tau(y)$ increases monotonically with y and that the response $R = R(y)$ decreases monotonically with y . The time difference is written as

$$\tau = t - s = \frac{s}{\ln(\kappa_2 s)} f(s, y) \quad (\text{C.3})$$

where the unknown function $f = f(s, y)$ plays the rôle of the scaling variable. We assume that $f \ln s \ll 1$. Then we can expand $R(t, s)$. After several cancellations, we finally arrive for the second model and third model, respectively, at

$$\ln R(t, s) \simeq \frac{\kappa_1}{16} f(s, y) - \frac{1}{2} \ln f(s, y) - \frac{1}{2} \ln(4\pi\nu s) + \frac{1}{2} \ln(\ln \kappa_2 s) + o(1) \quad (\text{C.4a})$$

$$\begin{aligned}\ln R(t, s) &\simeq \frac{f(s, y)}{16} \left(\kappa_1 - \frac{\ln \ln \kappa_2 s}{\ln \kappa_2 s} \right) - \frac{1}{2} \ln f(s, y) - \frac{1}{2} \ln(4\pi\nu s) + \frac{1}{2} \ln(\ln \kappa_2 s) + o(1) \\ &= \frac{\kappa_1 \bar{f}(s, y)}{16} - \frac{1}{2} \ln \bar{f}(s, y) - \frac{1}{2} \ln \left(1 - \frac{\ln \ln \kappa_2 s}{\kappa_1 \ln \kappa_2 s} \right) - \frac{1}{2} \ln(4\pi\nu s) + \frac{1}{2} \ln(\ln \kappa_2 s) + o(1) \\ &\simeq \frac{\kappa_1 \bar{f}(s, y)}{16} - \frac{1}{2} \ln \bar{f}(s, y) - \frac{1}{2} \ln(4\pi\nu s) + \frac{1}{2} \ln(\ln \kappa_2 s) + o(1)\end{aligned}\quad (\text{C.4b})$$

where for the third model we redefined the scaling variable $\bar{f}(s, y) := f(s, y) \left(1 - \frac{\ln \ln \kappa_2 s}{\kappa_1 \ln \kappa_2 s} \right) \stackrel{s \rightarrow \infty}{\simeq} f(s, y)$. The scaling of the autoresponse of the second model in (C.4a) and of the third model in (C.4b) can be discussed simultaneously, by using the scaling variables f or \bar{f} , respectively.

Now, we can *define* a scaling variable $y > 1$, for $s \rightarrow \infty$, through the ansatz (using f or \bar{f} , respectively)

$$\ln R(t, s) \stackrel{!}{=} -\frac{1}{2} \ln(4\pi\nu s) - \frac{1}{2} \ln(y-1) + \frac{B}{16} f(s, y) + A \ln(\ln \kappa_2 s) \quad (\text{C.5})$$

where A, B are constants. Consistency of (C.4, C.5) leads to

$$f(s, y) = \frac{8}{B - \kappa_1} W \left(\frac{B - \kappa_1}{8} (y-1) \ln^{1-2A}(\kappa_2 s) \right) \quad (\text{C.6})$$

where $2A > 1$, $B - \kappa_1 > 0$ and using again Lambert's function $W(x)$. For the third model, one simply reads \bar{f} instead of f . The response function becomes

$$\ln R(t, s) \simeq -\frac{1}{2} \ln(4\pi\nu s) + A \ln(\ln \kappa_2 s) - \frac{1}{2} \ln(y-1) + \frac{B}{16} \underbrace{\ln^{1-2A}(\kappa_2 s)}_{\rightarrow 0 \text{ for } s \rightarrow \infty} (y-1)$$

and we have the final scaling form, with $A > \frac{1}{2}$

$$R(t, s) = (4\pi\nu s)^{-1/2} \ln^A(\kappa_2 s) (y-1)^{-1/2} \quad (\text{C.7})$$

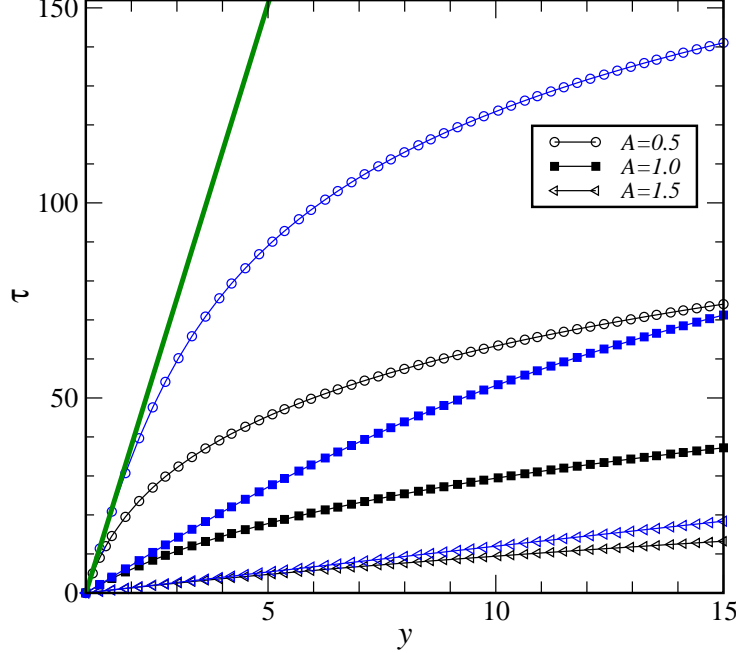


Figure 4: Illustration of the definition of the scaling variables $\tau = \tau(s, y)$, for fixed waiting time s . The black curves show the definition (4.17) for the response, for several values of $\vartheta = 2A$, and the blue curves correspond to (4.8) for the correlator. The straight green line is the asymptotic form $\tau = (y - 1)s / \ln s$.

with the scaling variable

$$t - s = \frac{s}{\ln \kappa_2 s} \frac{8}{B - \kappa_1} W \left(\frac{B - \kappa_1}{8} (y - 1) \ln^{1-2A}(\kappa_2 s) \right) \quad (\text{C.8})$$

such that for $s \rightarrow \infty$, we recover $t - s \simeq s \ln^{-2A}(\kappa_2 s) (y - 1)$ with $2A > 1$.

To finish the argument, we now compare with the scaling of the autocorrelator, discussed in appendix B. Because of the condition $2A > 1$, the scaling (C.8) cannot be compatible with (4.6). *A contrario*, compatibility with (4.8) can be achieved via the condition

$$2A = \frac{1 + \delta_{\kappa_1,3} - \kappa_1}{2} + A' + \vartheta \quad (\text{C.9})$$

It follows that the condition $2A > 1$ implies the bound $\kappa_1 - 2A' - 2\vartheta - \delta_{\kappa_1,3} < 0$ obtained in appendix B. Since we shall only encounter the combination $A' + \vartheta$, we may as well fix one of those two constants. For example, we might insist that the function f in (B.14) should not become singular for $s \rightarrow \infty$. This fixes $\kappa_1 - 2A' - 2\vartheta - \delta_{\kappa_1,3} = 0$, hence

$$\vartheta = 2A, \quad A' = \frac{1}{2}(\kappa_1 - 1 - \delta_{\kappa_1,3}) \quad (\text{C.10})$$

This produces the final forms (4.8) and (4.17) in the text, if we choose $B = \kappa_1 + 8$ and $B' = \kappa_1 - 16$. In figure 4 we compare the functions $\tau = \tau(s, y)$, for s finite and fixed, for responses and correlators. This illustrates that unless s becomes enormously large, there are strong non-linearities in the scaling variable to be taken into account.

Finally, the asymptotic form in (4.16) is derived in completely analogy with the treatment of the correlator in appendix B. The absence of a spatial modulation in (4.16) follows from

$$\frac{(Z(t) - Z(s))^2}{2\nu(t-s)} = O(\ln^{-1} s) \quad (\text{C.11})$$

Appendix D. On some special functions

We compute the functions \mathcal{J}_a , with $a \in \mathbb{N}$, defined by

$$\mathcal{J}_{2a}(A, Z) := \frac{1}{\pi} \int_0^\pi dk e^{A \cos k} \cosh(Z \sin k) (\sin k)^{2a} = \frac{\partial^{2a}}{\partial Z^{2a}} \mathcal{J}_0(A, Z) \quad (\text{D.1})$$

$$\mathcal{J}_{2a+1}(A, Z) := \frac{1}{\pi} \int_0^\pi dk e^{A \cos k} \sinh(Z \sin k) (\sin k)^{2a+1} = \frac{\partial^{2a+1}}{\partial Z^{2a+1}} \mathcal{J}_0(A, Z) \quad (\text{D.2})$$

and in principle, it is enough to find \mathcal{J}_0 explicitly. This can be done as follows

$$\begin{aligned} \mathcal{J}_0(A, Z) &= \frac{1}{\pi} \int_0^\pi dk e^{A \cos k} \sum_{r=0}^{\infty} \frac{Z^{2r}}{(2r)!} \sin^{2r} k \\ &= \sum_{r=0}^{\infty} \frac{1}{\pi} \frac{Z^{2r}}{\Gamma(2r+1)} \sqrt{\pi} \Gamma\left(r + \frac{1}{2}\right) \left(\frac{A}{2}\right)^{-r} I_r(A) \\ &= \sum_{r=0}^{\infty} \left(\frac{Z^2}{2A}\right)^r \frac{1}{r!} I_r(A) = \sum_{r=0}^{\infty} \left(\frac{A}{2}\right)^r \frac{I_r(A)}{r!} \left[\left(\frac{Z}{A}\right)^2\right]^r \\ &= I_0\left(A\sqrt{1 + Z^2/A^2}\right) = I_0\left(\sqrt{A^2 + Z^2}\right) \end{aligned} \quad (\text{D.3})$$

Herein, after expanding the cosh in the first line, we used an integral representation [1, eq. (9.6.18)] of the modified Bessel function $I_r(A)$ in the second line, simplified in the third line with the help of the duplication formula [1, eq. (6.1.18)] of the Gamma-function and in the forth line applied the multiplication formula [1, eq. (9.6.51)] for the I_r (see also (E.7) below).

We notice the unexpected rotation-symmetry, in the (A, Z) -plane, of the integral identity

$$\frac{1}{\pi} \int_0^\pi dk e^{A \cos k} \cosh(Z \sin k) = I_0\left(\sqrt{A^2 + Z^2}\right) \quad (\text{D.4})$$

just derived.

Similarly, one can express \mathcal{J}_1 , with the help of [1, eqs. (9.6.18, 6.1.18, 9.6.51)] as :

$$\begin{aligned} \mathcal{J}_1(A, Z) &= \frac{1}{\pi} \int_0^\pi dk e^{A \cos k} \sum_{r=0}^{\infty} \frac{Z^{2r}}{(2r)!} \sin^{2r+1} k \\ &= \sum_{r=0}^{\infty} \left(\frac{A}{2}\right)^r \left(\frac{Z}{A}\right)^{2r+1} \frac{I_{r+1}(A)}{r!} \\ &= \frac{Z I_1\left(\sqrt{A^2 + Z^2}\right)}{\sqrt{A^2 + Z^2}} \end{aligned} \quad (\text{D.5})$$

and one can also verify that $\mathcal{J}_1(A, Z) = \partial_Z \mathcal{J}_0(A, Z)$. Similarly, $\mathcal{J}_2(A, Z) = \partial_Z \mathcal{J}_1(A, Z)$.

Appendix E. Proof of an identity

We derive the following identity, for all $n \in \mathbb{N}$ and $A, Z \in \mathbb{C}$

$$\mathcal{C}_n(A, Z) := \frac{1}{\pi} \int_0^\pi dk e^{A \cos k} \cosh(Z \sin k) \cos(nk) = I_n \left(\sqrt{A^2 + Z^2} \right) \cos \left(n \arctan \left(\frac{Z}{A} \right) \right) \quad (\text{E.1})$$

where I_n is a modified Bessel function. The special case $n = 0$ is the function $\mathcal{J}_0(A, Z)$ derived in appendix D. For the proof, we shall require the following result:

Lemma: For any integers $n, \nu \in \mathbb{N}$ and $z, \mathfrak{z} \in \mathbb{C}$, one has

$$\frac{1}{\pi} \int_0^\pi d\theta \exp(z \cos \theta) \cos(n\theta) \sin^{2\nu} \theta = \frac{(-1)^\nu}{2^{2\nu}} \sum_{k=0}^{2\nu} (-1)^k \binom{2\nu}{k} I_{n+2\nu-2k}(z) \quad (\text{E.2})$$

$$\frac{1}{\pi} \int_0^\pi d\theta \exp(i\mathfrak{z} \cos \theta) \cos(n\theta) \sin^{2\nu} \theta = \frac{i^n}{2^{2\nu}} \sum_{k=0}^{2\nu} \binom{2\nu}{k} J_{n+2\nu-2k}(\mathfrak{z}) \quad (\text{E.3})$$

where J_n is a Bessel function and I_n is a modified Bessel function [1].

Corollary: Separating the real and imaginary parts in (E.3), for n even and odd, respectively, gives for $\mathfrak{z} \in \mathbb{R}$ ($m, \nu \in \mathbb{N}$)

$$\begin{aligned} \frac{1}{\pi} \int_0^\pi d\theta \cos(\mathfrak{z} \cos \theta) \cos(2m\theta) \sin^{2\nu} \theta &= \frac{(-1)^m}{2^{2\nu}} \sum_{k=0}^{2\nu} \binom{2\nu}{k} J_{2m+2\nu-2k}(\mathfrak{z}) \\ \frac{1}{\pi} \int_0^\pi d\theta \sin(\mathfrak{z} \cos \theta) \cos((2m+1)\theta) \sin^{2\nu} \theta &= \frac{(-1)^m}{2^{2\nu}} \sum_{k=0}^{2\nu} \binom{2\nu}{k} J_{2m+1+2\nu-2k}(\mathfrak{z}) \\ \int_0^\pi d\theta \sin(\mathfrak{z} \cos \theta) \cos(2m\theta) \sin^{2\nu} \theta &= \int_0^\pi d\theta \cos(\mathfrak{z} \cos \theta) \cos((2m+1)\theta) \sin^{2\nu} \theta = 0 \end{aligned}$$

The strategy of proof will be as follows: (E.1) follows from (E.2), which in turn is an immediate consequence of (E.3).

Step 1: To prove (E.3), recall Euler's formula, $e^{i\mathfrak{z} \cos \theta} = \cos(\mathfrak{z} \cos \theta) + i \sin(\mathfrak{z} \cos \theta)$, with $\mathfrak{z} \in \mathbb{C}$. Multiplying with $\cos n\theta$ and integrating gives, see [1, eq. (9.1.21)], with $n \in \mathbb{N}$

$$i^n J_n(\mathfrak{z}) = \frac{1}{\pi} \int_0^\pi d\theta \cos(\mathfrak{z} \cos \theta) \cos(n\theta) + \frac{i}{\pi} \int_0^\pi d\theta \sin(\mathfrak{z} \cos \theta) \cos(n\theta) \quad (\text{E.4})$$

Next, denote the integral on the left-hand-side of (E.3) as $C_{n,\nu}(\mathfrak{z}) := \frac{1}{\pi} \int_0^\pi d\theta e^{i\mathfrak{z} \cos \theta} \cos(n\theta) \sin^{2\nu} \theta$. It is easily verified that one has the differential recurrence relation

$$C_{n,\nu+1}(\mathfrak{z}) = \partial_{\mathfrak{z}}^2 C_{n,\nu}(\mathfrak{z}) + C_{n,\nu}(\mathfrak{z}) \quad (\text{E.5})$$

For a fixed $n \in \mathbb{N}$, the identity (E.3) is the assertion that for all $\nu \in \mathbb{N}$ one has the identity:

$$C_{n,\nu}(\mathfrak{z}) = \frac{i^n}{2^{2\nu}} \sum_{k=0}^{2\nu} \binom{2\nu}{k} J_{n+2\nu-2k}(\mathfrak{z}) \quad (\text{E.6})$$

which we now prove by induction over ν . For $\nu = 0$, the assertion (E.6) is just the relation (E.4). For the induction step $\nu \mapsto \nu + 1$, we use¹⁶ (E.5) and apply first the Bessel function identities [1, eq. (9.1.27)] and then several times standard identities of the binomial coefficients

$$\begin{aligned}
C_{n,\nu+1}(\mathfrak{z}) &= \left(1 + \frac{\partial^2}{\partial \mathfrak{z}^2}\right) C_{n,\nu}(\mathfrak{z}) \\
&= \frac{i^n}{2^{2\nu}} \sum_{k=0}^{2\nu} \binom{2\nu}{k} \left[J_{n+2\nu-2k} + \frac{1}{4} [J_{n-2+2\nu-2k} - 2J_{n+2\nu-2k} + J_{n+2+2\nu-2k}] \right] \\
&= \frac{i^n}{2^{2(\nu+1)}} \sum_{k=0}^{2\nu} \binom{2\nu}{k} \left[J_{n+2\nu-2k} + J_{n-2+2\nu-2k} + J_{n+2+2\nu-2k} + J_{n+2\nu-2k} \right] \\
&= \frac{i^n}{2^{2(\nu+1)}} \left\{ \sum_{k=0}^{2\nu} \binom{2\nu}{k} J_{n+2\nu-2k} + \sum_{k=1}^{2\nu+1} \binom{2\nu}{k-1} J_{n+2\nu-2k} \right. \\
&\quad \left. + \sum_{k=0}^{2\nu} \binom{2\nu}{k} J_{n+2(\nu+1)-2k} + \sum_{k=1}^{2\nu+1} \binom{2\nu}{k-1} J_{n+2(\nu+1)-2k} \right\} \\
&= \frac{i^n}{2^{2(\nu+1)}} \left\{ J_{n+2\nu} + \sum_{k=1}^{2\nu} \binom{2\nu+1}{k} J_{n+2\nu-2k} + J_{n+2\nu-2(2\nu+1)} \right. \\
&\quad \left. + J_{n+2(\nu+1)} + \sum_{k=1}^{2\nu} \binom{2\nu+1}{k} J_{n+2(\nu+1)-2k} + J_{n+2(\nu+1)-2(2\nu+1)} \right\} \\
&= \frac{i^n}{2^{2(\nu+1)}} \left\{ J_{n+2\nu} + J_{n-2(\nu+1)} + J_{n+2(\nu+1)} + J_{n-2\nu} \right. \\
&\quad \left. + \sum_{k=2}^{2\nu+1} \binom{2\nu+1}{k-1} J_{n+2(\nu+1)-2k} + \sum_{k=1}^{2\nu} \binom{2\nu+1}{k} J_{n+2(\nu+1)-2k} \right\} \\
&= \frac{i^n}{2^{2(\nu+1)}} \left\{ J_{n+2\nu} + J_{n+2(\nu+1)} + J_{n-2(\nu+1)} + J_{n-2\nu} + (2\nu+1)J_{n+2\nu} + (2\nu+1)J_{n-2\nu} \right. \\
&\quad \left. + \sum_{k=2}^{2\nu} \binom{2\nu+2}{k} J_{n+2(\nu+1)-2k} \right\} \\
&= \frac{i^n}{2^{2(\nu+1)}} \sum_{k=0}^{2(\nu+1)} \binom{2(\nu+1)}{k} J_{n+2(\nu+1)-2k}(\mathfrak{z})
\end{aligned}$$

which proves the assertion (E.6) for all $\nu \in \mathbb{N}$ (in the last line, we restored the argument \mathfrak{z}).

Step 2: starting from (E.3), it is enough to set $\mathfrak{z} = iz$ and to recall that $J_n(iz) = i^n I_n(z)$. Eq. (E.3) then gives

$$\frac{1}{\pi} \int_0^\pi d\theta e^{-z \cos \theta} \cos(n\theta) \sin^{2\nu} \theta = \frac{(-1)^{n+\nu}}{2^{2\nu}} \sum_{k=0}^{2\nu} \binom{2\nu}{k} (-1)^k I_{n+2\nu-2k}(z).$$

Going over to $z \mapsto -z$, along with $I_n(-z) = (-1)^n I_n(z)$, produces (E.2). This proves the lemma.

¹⁶In this calculation, we write J_n instead of fully $J_n(\mathfrak{z})$.

Step 3: For proving (E.1), we require two more preparations. First, recall the identity [1, eq. (9.6.51)], for $n \in \mathbb{N}$, $x \in \mathbb{C}$ and $\lambda \neq 0$

$$\sum_{\ell=0}^{\infty} \frac{(\lambda^2 - 1)^\ell (x/2)^\ell}{\ell!} I_{n \pm \ell}(x) = \lambda^{\mp n} I_n(\lambda x) \quad (\text{E.7})$$

Second, let $x = \tan \varphi$. Then

$$\left(\frac{1 - ix}{1 + ix} \right)^{n/2} + \left(\frac{1 + ix}{1 - ix} \right)^{n/2} = \exp \left(-2i\varphi \frac{n}{2} \right) + \exp \left(+2i\varphi \frac{n}{2} \right) = 2 \cos n\varphi \quad (\text{E.8})$$

Now, denote the left-hand-side of (E.1) by $\mathcal{C}_n = \mathcal{C}_n(A, Z)$. Expanding the cosh in the integral representation of \mathcal{C}_n , we have

$$\begin{aligned} \mathcal{C}_n &= \frac{1}{\pi} \sum_{m=0}^{\infty} \frac{Z^{2m}}{(2m)!} \int_0^\pi dk e^{A \cos k} \sin^{2m} k \cos(kn) \\ &= \sum_{m=0}^{\infty} \sum_{\ell=0}^{2m} \left(\frac{Z}{2} \right)^{2m} \frac{(-1)^{m+\ell}}{(2m-\ell)! \ell!} I_{n+2m-2\ell}(A) \\ &= \sum_{m=0}^{\infty} \sum_{\ell=0}^m \frac{1}{2} \left[1 + (-1)^m \right] \left(\frac{Z}{2} \right)^m \frac{i^m (-1)^\ell}{(m-\ell)! \ell!} I_{n+m-2\ell}(A) \end{aligned}$$

where in the second line, we used (E.2). In the last line, we replaced the even integer $2m$ by the integer $m \in \mathbb{N}$, where the extra factor guarantees that only the even values of m give a non-vanishing contribution. Now, we can exchange the order of summation and perform afterwards

a shift in the summation variable m , to obtain

$$\begin{aligned}
\mathcal{C}_n &= \sum_{\ell=0}^{\infty} \sum_{m=\ell}^{\infty} \frac{1}{2} \left[1 + (-1)^m \right] \left(\frac{Z}{2} \right)^m \frac{i^m (-1)^\ell}{(m-\ell)! \ell!} I_{n+m-2\ell}(A) \\
&= \frac{1}{2} \sum_{\ell=0}^{\infty} \sum_{m=0}^{\infty} \left[(-1)^\ell + (-1)^{m+\ell} \right] \left(\frac{iZ}{2} \right)^{m+\ell} \frac{1}{m! \ell!} I_{n-\ell+m}(A) \\
&= \frac{1}{2} \sum_{\ell=0}^{\infty} \frac{1}{\ell!} \left(\frac{iZ}{2} \right)^\ell \sum_{m=0}^{\infty} \left[(-1)^\ell + (-1)^{m+\ell} \right] \frac{1}{m!} \left(\frac{A}{2} \right)^m \left(\frac{A}{2} \right)^m I_{(n-\ell)+m}(A) \\
&= \frac{1}{2} \sum_{\ell=0}^{\infty} \frac{1}{\ell!} \left(\frac{iZ}{2} \right)^\ell \left[(-1)^\ell \left(1 + i \frac{Z}{A} \right)^{-(n-\ell)/2} I_{n-\ell} \left(A \sqrt{1 + i \frac{Z}{A}} \right) \right. \\
&\quad \left. + \left(1 - i \frac{Z}{A} \right)^{-(n-\ell)/2} I_{n-\ell} \left(A \sqrt{1 - i \frac{Z}{A}} \right) \right] \\
&= \frac{1}{2} \left(1 + i \frac{Z}{A} \right)^{-n/2} \sum_{\ell=0}^{\infty} \frac{1}{\ell!} \left(-i \frac{Z}{A} \right)^\ell \left(\frac{1}{2} A \sqrt{1 + i \frac{Z}{A}} \right)^\ell I_{n-\ell} \left(A \sqrt{1 + i \frac{Z}{A}} \right) \\
&\quad + \frac{1}{2} \left(1 - i \frac{Z}{A} \right)^{-n/2} \sum_{\ell=0}^{\infty} \frac{1}{\ell!} \left(i \frac{Z}{A} \right)^\ell \left(\frac{1}{2} A \sqrt{1 - i \frac{Z}{A}} \right)^\ell I_{n-\ell} \left(A \sqrt{1 - i \frac{Z}{A}} \right) \\
&= \frac{1}{2} \left[\left(\frac{1 - iZ/A}{1 + iZ/A} \right)^{n/2} + \left(\frac{1 + iZ/A}{1 - iZ/A} \right)^{n/2} \right] I_n \left(A \sqrt{1 + \frac{Z^2}{A^2}} \right) \\
&= \cos \left(n \arctan \frac{Z}{A} \right) I_n \left(\sqrt{A^2 + Z^2} \right)
\end{aligned}$$

as asserted. In the calculation, we applied in the third and fifth lines the identity (E.7), to carry out, first the sum over m , and then over ℓ , and finally used (E.8) in the seventh line.

Appendix F. Discrete cosine- and sine-transformations

For the convenience of the reader, we recall some basic properties of discrete cosine and sine transformations. On a periodic chain with N sites, the cosine-transformation \mathcal{C} of an even function $a_n(t) = a_{-n}(t)$ is defined as, with $k = 0, 1, \dots, N-1$

$$\widehat{a}(t, k) = \mathcal{C}(a_n(t))(k) := \sum_{n=0}^{N-1} \cos \left(\frac{2\pi}{N} kn \right) a_n(t) \quad , \quad a_n(t) = \frac{1}{N} \sum_{k=0}^{N-1} \cos \left(\frac{2\pi}{N} kn \right) \widehat{a}(t, k) \quad (\text{F.1})$$

and is itself even, viz. $\widehat{a}(t, k) = \widehat{a}(t, -k)$. The sine-transformation \mathcal{S} of an odd function $b_n(t) = -b_{-n}(t)$ is defined as

$$\widehat{b}(t, k) = \mathcal{S}(b_n(t))(k) := \sum_{n=0}^{N-1} \sin \left(\frac{2\pi}{N} kn \right) b_n(t) \quad , \quad b_n(t) = \frac{1}{N} \sum_{k=0}^{N-1} \sin \left(\frac{2\pi}{N} kn \right) \widehat{b}(t, k) \quad (\text{F.2})$$

and is itself odd, viz. $\widehat{b}(t, k) = -\widehat{b}(t, -k)$. Clearly, \mathcal{C} and \mathcal{S} are linear operators. Furthermore, $\mathcal{C}(b_n(t)) = \mathcal{S}(a_n(t)) = 0$ and $\mathcal{C}^2(a_n(t)) = Na_n(t)$ and $\mathcal{S}^2(b_n(t)) = Nb_n(t)$.

In the main text, we shall need frequently the following cosine-transformations of the even functions

$$\begin{aligned}\mathcal{C}(a_{n+1}(t) + a_{n-1}(t) - 2a_n(t))(k) &= \sum_{n=0}^{N-1} \cos\left(\frac{2\pi}{N}kn\right) (a_{n+1}(t) + a_{n-1}(t) - 2a_n(t)) \\ &= -2 \left[1 - \cos \frac{2\pi}{N}k\right] \widehat{a}(t, k)\end{aligned}\tag{F.3}$$

$$\begin{aligned}\mathcal{C}\left(\frac{1}{2}(b_{n+1}(t) - b_{n-1}(t))\right)(k) &= \frac{1}{2} \sum_{n=0}^{N-1} \cos\left(\frac{2\pi}{N}kn\right) (b_{n+1}(t) - b_{n-1}(t)) \\ &= \sin\left(\frac{2\pi}{N}k\right) \widehat{b}(t, k)\end{aligned}\tag{F.4}$$

and also the sine-transformations of the odd functions

$$\begin{aligned}\mathcal{S}(b_{n+1}(t) + b_{n-1}(t) - 2b_n(t))(k) &= \sum_{n=0}^{N-1} \sin\left(\frac{2\pi}{N}kn\right) (b_{n+1}(t) + b_{n-1}(t) - 2b_n(t)) \\ &= -2 \left[1 - \cos \frac{2\pi}{N}k\right] \widehat{b}(t, k)\end{aligned}\tag{F.5}$$

$$\begin{aligned}\mathcal{S}\left(\frac{1}{2}(a_{n+1}(t) - a_{n-1}(t))\right)(k) &= \frac{1}{2} \sum_{n=0}^{N-1} \sin\left(\frac{2\pi}{N}kn\right) (a_{n+1}(t) - a_{n-1}(t)) \\ &= -\sin\left(\frac{2\pi}{N}k\right) \widehat{a}(t, k)\end{aligned}\tag{F.6}$$

Acknowledgements: MH is grateful to KIAS Séoul for warm hospitality, where a large part of this work was done. We thank N. Allegra, L. Berthier, J.-Y. Fortin, H. Park, U.C. Täuber and M. Zannetti for useful discussions and/or correspondence. This work was also partly supported by the Collège Doctoral franco-allemand Nancy-Leipzig-Coventry (*‘Systèmes complexes à l’équilibre et hors équilibre’*) of UFA-DFH and also by the National Research Foundation of Korea (NRF) grant funded by the Korea government (MSIP) (No. 2016R1A2B2013972).

References

- [1] M. Abramowitz and I.A. Stegun, *Handbook of Mathematical Functions*, Dover (New York 1965)
- [2] S. Atis, S. Saha, H. Auradou, S. Salin, L. Talon, Phys. Rev. Lett. **110**, 148301 (2013) [[arXiv:1210.3518](#)];
S. Atis, A.K. Dubey, D. Salin, L. Talon, P. Le Doussal, K.J. Wiese, Phys. Rev. Lett. **114**, 234502 (2015) [[arXiv:1410.1097](#)].
- [3] A.L. Barabási and H.E. Stanley, *Fractal concepts in surface growth*, Cambridge University Press (1995).
- [4] E. ben-Naim and P.L. Krapivsky, J. Phys. **A45**, 455003 (2012) [[arXiv:1209.0043](#)].
- [5] A.J. Bray and K. Humayun, Phys. Rev. Lett. **68**, 1559 (1992).

- [6] A.J. Bray, Adv. Phys. **43**, 357 (1994).
- [7] T.H. Berlin and M. Kac, Phys. Rev. **86**, 821 (1952).
- [8] L. Bertini and G. Giacomin, Comm. Math. Phys. **183**, 571 (1997).
- [9] L. Berthier, Eur. Phys. J. **B17**, 689 (2000) [arxiv:cond-mat/0003122].
- [10] J.M. Burgers, *The nonlinear diffusion equation: asymptotic solutions and statistical problems*, Reidel (Dordrecht 1974).
- [11] S. Bustingorry, J. Stat. Mech. P10002 (2007) [arXiv:0708.2615].
- [12] P. Calabrese and P. Le Doussal, Phys. Rev. Lett. **106**, 250603 (2011) [arXiv:1104.1993].
- [13] P. Calabrese, M. Kormos and P. Le Doussal, Europhys. Lett. **107**, 10011 (2014) [arXiv:1405.2582].
- [14] A. Coniglio and M. Zannetti, Europhys. Lett. **10**, 575 (1989);
A. Coniglio, P. Ruggiero and M. Zanetti, Phys. Rev. **E50**, 1046 (1994).
- [15] A. Coniglio and M. Zannetti, Physica **A163**, 325 (1990);
C. Amitrano, A. Coniglio, P. Meakin, M. Zannetti, Fractals **1**, 840 (1993).
- [16] R.M. Corless, G.H. Gonnet, D.E.G. Hare, D.J. Jeffrey, D.E. Knuth, Adv. Compt. Math. **5**, 329 (1996).
- [17] I. Corwin, Rand. Matrices Theory Appl. **1**, 1130001 (2012) [arXiv:1106.1596].
- [18] L.F. Cugliandolo and J. Kurchan, J. Phys. **A27**, 5749 (1994) [cond-mat/9311016];
L.F. Cugliandolo, J. Kurchan and G. Parisi, J. Physique **I4**, 1641 (1994) [cond-mat/9406053].
- [19] L.F. Cugliandolo and D. Dean, J. Phys. **A28**, 4213 (1995) [cond-mat/9502075].
- [20] L.F. Cugliandolo, in J.-L. Barrat, M. Feiglman, J. Kurchan, J. Dalibard (eds), *Slow relaxations and non-equilibrium dynamics in condensed matter*, Les Houches LXXVII, Springer (Heidelberg 2003), pp. 367-521 [cond-mat/0210312].
- [21] G.L. Daquila and U.C. Täuber, Phys. Rev. **E83**, 051107 (2011) [arXiv:1102.2824].
- [22] S.B. Dutta, J. Phys. **A41**, 395002 (2008) [arXiv:0806.3642].
- [23] S.F. Edwards and D.R. Wilkinson, Proc. Roy. Soc. **A381**, 17 (1982).
- [24] F. Family and T. Vicsek, J. Phys. **A18**, L75 (1985).
- [25] W. Feller, *An introduction to probability theory and its applications*, vol. 2 (2nd ed), Wiley (New York 1971).
- [26] J.-Y. Fortin and S. Mantelli, J. Phys. **A45**, 475001 (2012) [arXiv:1208.2114].
- [27] N. Fusco and M. Zannetti, Phys. Rev. **E66**, 066113 (2002) [cond-mat/0210502].
- [28] Y.V. Fyodorov, A. Perret and G. Schehr, J. Stat. Mech. P11017 (2015) [arXiv:1507.08520].
- [29] C. Godrèche and J.-M. Luck, J. Phys. **A33**, 9141 (2000) [cond-mat/0001264].
- [30] C. Godrèche and J.-M. Luck, J. Stat. Mech. P05006 (2013) [arXiv:1302.4658].

- [31] L.-H. Gwa and H. Spohn, Phys. Rev. **A46**, 844 (1992).
- [32] T. Halpin-Healy and Y.-C. Zhang, Phys. Rep. **254**, 215 (1995).
- [33] T. Halpin-Healy, Phys. Rev. Lett. **109**, 170602 (2012).
- [34] T. Halpin-Healy, Phys. Rev. **E88**, 042118 (2013); erratum **E88**, 069903(E) (2013).
- [35] T. Halpin-Healy and Y. Lin, Phys. Rev. **E89**, 010103(R) (2014) [arXiv:1310.8013].
- [36] T. Halpin-Healy and G. Palasantzas, Europhys. Lett. **105**, 50001 (2014) [arXiv:1403.7509].
- [37] M. Henkel and M. Pleimling, “*Non-equilibrium phase transitions vol. 2: ageing and dynamical scaling far from equilibrium*”, Springer (Heidelberg 2010).
- [38] M. Henkel, J.D. Noh and M. Pleimling, Phys. Rev. **E85**, 030102(R) (2012) [arXiv:1109.5022].
- [39] M. Henkel and X. Durang, J. Stat. Mech. P05022 (2015) [arXiv:1501.07745].
- [40] M.A.C. Huergo, M.A. Pasquale, A.E. Bolzán, A.J. Arvia and P.H. González, Phys. Rev. **E82**, 031903 (2010);
M.A.C. Huergo, M.A. Pasquale, P.H. González, A.E. Bolzán and A.J. Arvia, Phys. Rev. **E84**, 021917 (2011);
M.A.C. Huergo, M.A. Pasquale, P.H. González, A.E. Bolzán and A.J. Arvia, Phys. Rev. **E85**, 011918 (2012).
- [41] M.A.C. Huergo, N.E. Muzzio, M.A. Pasquale, P.H. González, A.E. Bolzán and A.J. Arvia, Phys. Rev. **E90**, 022706 (2014).
- [42] J.L. Iguain, S. Bustingorry, A.B. Kolton, L.F. Cugliandolo, Phys. Rev. **B80**, 094201 (2009) [arXiv:0903.4878];
S. Bustingorry, L.F. Cugliandolo and J.L. Iguain, J. Stat. Mech. P09008 (2007) [arXiv:0705.3348].
- [43] T. Imamura and T. Sasamoto, Phys. Rev. Lett. **108**, 190603 (2014) [arXiv:1111.4634];
J. Stat. Phys. **150**, 908 (2013) [arXiv:1210.4278].
- [44] G.S. Joyce, in C. Domb and M.S. Green (eds) *Phase transitions and critical phenomena*, Vol. 2, Academic Press (London 1972), pp. 375ff.
- [45] H. Kallabis and J. Krug, Europhys. Lett. **45**, 20 (1999) [cond-mat/9809241].
- [46] M. Kardar, G. Parisi and Y.-C. Zhang, Phys. Rev. Lett. **56**, 889 (1986).
- [47] J. Kelling, G. Ódor and S. Gemming, J. Phys. **A50**, 12LT01 (2017) [arXiv:1605.02620].
- [48] J. Kelling, G. Ódor and S. Gemming, [arXiv:1701.03638].
- [49] J. Kelling, G. Ódor and S. Gemming, Comp. Phys. Comm. **220**, 205 (2017) [arXiv:1705.01022].
- [50] R. Kenna, D.C. Johnston, W. Janke, Phys. Rev. Lett. **96**, 115701 (2006) [arxiv:cond-mat/0605162];
R. Kenna, D.C. Johnston, W. Janke, Phys. Rev. Lett. **97**, 155702 (2006) [arxiv:cond-mat/0608127]; erratum Phys. Rev. Lett. **97** (2006) 169901 (2006);
R. Kenna, in Yu. Holovatch (ed) *Order, Disorder and Criticality: Advanced Problems of Phase Transition Theory*, vol. 3, World Scientific (Singapour 2013), p. 1 [arXiv:1205.4252].

- [51] M. Krech, Phys. Rev. **E55**, 668 (1997) [[cond-mat/9609230](#)]; erratum **E56**, 1285 (1997).
- [52] T. Kriecherbauer and J. Krug, J. Phys. **A43**, 403001 (2010) [[arXiv:0803.2796](#)].
- [53] J. Krug, Adv. Phys. **46**, 139 (1997).
- [54] J. Kurchan, Phys. Rev. **E66**, 017101 (2002) [[arxiv:cond-mat/0110628](#)].
- [55] J.H. Lambert, Acta Helv. **3**, 128 (1758);
 L. Euler, Acta Acad. Scient. Petropol. **II**, 29 (1779) [paper E532, printed 1783] and *Opera Omnia, Series Prima*, vol. 6, Teubner (Leipzig 1921);
 G. Polya und G. Szegő, *Aufgaben und Lehrsätze aus der Analysis*, 2 Bände, 4. Auflage, Springer (Heidelberg 1970/71);
 G. Polya and G. Szegő, *Problems and theorems in analysis* 2 vols., 5th ed., Springer (New York 1998).
- [56] T. Liggett, *Interacting particle systems*, Springer (Heidelberg 1985).
- [57] H.W. Lewis and G.H. Wannier, Phys. Rev. **88**, 682 (1952); erratum **90**, 1131 (1953).
- [58] K. Mallick, Physica **A418**, 17 (2015) [[arXiv:1412.6258](#)].
- [59] G.F. Mazenko, *Non-equilibrium statistical mechanics*, Wiley (New York 2006).
- [60] A. Menshutin, Phys. Rev. Lett. **108**, 015501 (2012).
- [61] F. Mohammadi, A.A. Saberi, S. Rouhani, J. Phys. Cond. Matt. **21**, 375110 (2009) [[arXiv:0905.0820](#)].
- [62] G. Ódor, J. Kelling, S. Gemming, Phys. Rev. **E89**, 032146 (2014) [[arXiv:1312.6029](#)].
- [63] Y. Oono and S. Puri, Mod. Phys. Lett. **B2**, 861 (1988).
- [64] A. Pagnani, G. Parisi, Phys. Rev. **E92**, 010101(R) (2015) [[arXiv:1611.08445](#)].
- [65] A. Picone and M. Henkel, J. Phys. **A35**, 5575 (2002) [[cond-mat/0203411](#)].
- [66] M. Prähofer, H. Spohn, Physica **A279**, 342 (2000) [[arXiv:cond-mat/9910273](#)].
- [67] G. Ronca, J. Chem. Phys. **68**, 3737 (1978).
- [68] A. Röthlein, F. Baumann and M. Pleimling, Phys. Rev. **E74**, 061604 (2006) [[cond-mat/0609707](#)]; erratum **E76**, 019901(E) (2007).
- [69] T. Sasamoto and H. Spohn, Phys. Rev. Lett. **104**, 230602 (2010) [[arXiv:1002.1883](#)].
- [70] S. Singh, R.K. Pathria, Phys. Rev. **B31**, 4483 (1985).
- [71] E. Somfai, R.C. Ball, N.E. Bowler, L.M. Sander, Physica **A325**, 19 (2003) [[arxiv:cond-mat/0210637](#)].
- [72] L.C.E. Struik, *Physical ageing in amorphous polymers and other materials*, Elsevier (Amsterdam 1978).
- [73] K.A. Takeuchi, M. Sano, T. Sasamoto and H. Spohn, Sci. Reports **1**:34 (2011) [[arXiv:1108.2118](#)];
 K.A. Takeuchi and M. Sano, Phys. Rev. Lett. **104**, 230601 (2010) [[arXiv:1001.5121](#)].

- [74] K.A. Takeuchi and M. Sano, J. Stat. Phys. **147**, 853 (2012) [[arXiv:1203.2530](#)].
- [75] K.A. Takeuchi, J. Stat. Mech. P01006 (2014) [[arXiv:1310.0220](#)].
- [76] K.A. Takeuchi, [[arXiv:1708.06060](#)].
- [77] U.C. Täuber, *Critical dynamics: a field-theory approach to equilibrium and non-equilibrium scaling behavior*, Cambridge University Press (Cambridge 2014).
- [78] U.C. Täuber, Ann. Rev. Cond. Matter Phys. **8**, 1 (2017) [[arXiv:1604.04487](#)].
- [79] E. Vincent, in M. Henkel, M. Pleimling, R. Sanctuary (eds) *Ageing and the glass transition*, Springer Lecture Notes in Physics **716**, Springer (Heidelberg 2007), p. 1, [[arxiv:cond-mat/0603583](#)].
- [80] S. Wald, G.T. Landi, M. Henkel, J. Stat. Mech. (at press) [[arXiv:1707.06273](#)].
- [81] H. Wio, R.R. Deza, C. Escudero, J.A. Revelli, Papers in Phys. **5**, 050010 (2013) [[arXiv:1401.6425](#)].
- [82] H. Wio, M.A. Rodriguez, R. Gallego, J.A. Revelli, A. Alés, R.R. Deza, Frontiers in Physics **4**, 52 (2017).
- [83] P.J. Yunker, M.A. Lohr, T. Still, A. Borodin, D.J. Durian, A.G. Yodh, Phys. Rev. Lett. **110**, 035501 (2013) [[arXiv:1209.4137](#)];
 Comment: M. Nicoli, R. Cuerno, M. Castro, Phys. Rev. Lett. **111**, 209601 (2013); P.J. Yunker *et al.*, Phys. Rev. Lett. **111**, 209602 (2013).